Transformative Technology for FLASH Radiation Therapy: A Snowmass 2021 White Paper

S. Boucher[1], E. Esarey[2], C.G.R. Geddes[2], C. Johnstone[3], S. Kutsaev[1], B.W. Loo Jr.[4], F. Méot[5], B. Mustapha[6], K. Nakamura[2], E. Nanni[9], L. Obst-Huebl[2], S.E. Sampayan[7], C. Schroeder[2], R. Schulte[8], K. Sheng[9], A. Snijders[2], E. Snively[10], S.G. Tantawi[10], J. van Tilborg[2]

[1] RadiaBeam Technologies, LLC, Santa Monica, CA 90404, USA

[2] Lawrence Berkeley National Laboratory, CA, 94720, USA

[3] Fermi National Accelerator Laboratory, Batavia, IL, 60510, USA

[4] Stanford University School of Medicine, Stanford, CA 94305, USA

[5] Brookhaven National Laboratory, Upton, NY 11973, USA

[6] Argonne National Laboratory, Lemont, IL 60439, USA

[7] Lawrence Livermore National Laboratory, Livermore, CA 94551, USA; and Opcondys, Inc., Manteca, CA 95336, USA

[8] Loma Linda University, Loma Linda, CA 92350, USA

[9] University of California, Los Angeles, CA 90095, USA

[10] SLAC National Accelerator Laboratory, Menlo Park, CA 94025, USA

Keywords: Accelerators, FLASH effect, Radiation Therapy

Abstract

Conventional cancer therapies include surgery, radiation therapy, chemotherapy, and, more recently, immunotherapy. These modalities are often combined to improve the therapeutic index. The general concept of radiation therapy is to increase the therapeutic index by creating a physical dose differential between tumors and normal tissues through precision dose targeting, image guidance, and high radiation beams that deliver radiation dose with high conformality, e.g., protons and ions. However, treatment and cure are still limited by normal tissue radiation toxicity, with many patients experiencing acute and long-term side effects. Recently, however, a fundamentally different paradigm for increasing the therapeutic index of radiation therapy has emerged, supported by preclinical research, and based on the FLASH radiation effect. FLASH radiation therapy (FLASH-RT) is an ultra-high dose-rate delivery of a therapeutic radiation dose within a fraction of a second. Experimental studies have shown that normal tissues seem to be universally spared at these high dose rates, whereas tumors are not. The dose delivery conditions are not yet fully characterized. Still, it is currently estimated that large doses ($\geq$10 Gy) delivered in 200 ms or less produce normal tissue sparing effects yet effectively kill tumor cells. There is a great opportunity, but also many technical challenges, for the accelerator community to create the required dose rates with novel and compact accelerators to ensure the safe delivery of FLASH radiation beams.

.

1 Introduction

Radiation therapy is a dynamic research field driven by new technology developments. An exciting recent discovery is the sparing of normal (non-tumor) tissues when irradiated with ultra-high dose rates, but tumors are not spared when irradiated with the same radiation field, as first reported by Favaudon and colleagues in 2014 [1]. This phenomenon, which is now called the FLASH effect, opens up a potential new modality in radiation therapy (RT). Tissue sparing means that much higher radiation doses than conventional ones are tolerated increasing the potential for a cure with an accompanying reduction in side effects.

Many preclinical and first clinical results indicate a dramatic reduction of toxicity response at FLASH-RT dose rates compared to conventional dose rates. The first human patient treated with FLASH 2019 (a patient with recurrent cutaneous T-cell lymphoma) had a complete response with minimal skin toxicity despite being previously and repeatedly treated with conventional photon and electron RT at the tumor site [2]. FLASH-RT produced a complete response and was exceptionally tolerated even after multiple non-FLASH skin irradiations had produced significant radiation damage from both photons and electrons.

Most FLASH experiments and preclinical studies have been performed with electrons and only very few with protons. However, conventional radiotherapeutic electron beams (4-25 MeV) cannot penetrate enough to treat deep-seated tumors and are thus not likely to be widely used clinically for FLASH-RT. The distal dose fall-off of electrons in tissue is quite shallow as electrons are scattered and have considerable energy straggling, especially at low energies. Protons are currently the most commonly used heavy-charged particle in RT with a Bragg peak dose and finite range advantage. They are also beginning to be used for the first treatment planning studies for

clinical trials with FLASH-RT [3, 4]. Heavy ions, like carbon and helium, are not widely used despite a potentially much greater therapeutic effect due to high linear energy transfer (LET). The high associated costs of ion accelerator and gantry technologies have prevented widespread use. However, several carbon ion facilities are operational in Europe and Asia, particularly Japan.

Considerable research and development in this area is essential to optimize and clinically realize the curative potential of FLASH-RT with different radiation modalities. Currently, electron FLASH studies are performed using 4-6 MeV electron beams from modified clinical linacs and provide the strongest, most consistent preclinical evidence for the FLASH effect. Experimental high dose rate photon beams have been formed using synchrotron radiation and keV X-rays from a tube (very early FLASH-RT studies) with mixed results for the FLASH effect. The FLASH effect has also been observed with protons using shoot-through beams from clinical CW or iso-cyclotrons. In shoot-through beams, the beam is not energy degraded, so the proton energy ranges from 230-250 MeV, i.e., the highest available proton energy with these cyclotrons. Once energy degraders are introduced into the beam to create lower energy proton beams, FLASH intensities cannot be achieved. Synchrotrons, even the rapid cycling 15 Hz ion synchrotron being developed at BNL, cannot produce the intense ion beams required for a clinical application of FLASH-RT– and only a very small volume can be irradiated at the cycle time of the synchrotron.

2 Beam conditions for the FLASH Effect

Preclinical electron studies have generated a self-consistent set of general beam conditions for FLASH as >40Gy/sec, >10 Gy delivered in <250 ms, with an instantaneous dose rate >10^6 Gy/sec instantaneous dose rate during a microsecond beam pulse [5-7]. The instantaneous dose rate

requirement appears to be of particular significance as it has been observed across all radiation modalities, as summarized in Figure 1. The two proton outliers may reflect a difference between the beam structure of the quasi-continuous wave (CW) proton therapy beam and the 100-300 Hz pulsed electron beam, which has an RF bunch microstructure. The RF GHz bunch microstructure of the electron beam is approximately two orders of magnitude shorter than the MHz RF bunch structure of the proton beam. How these different time structures influence the observation of a FLASH effect is unclear as systematic studies of pulse duration and frequency in different biological systems have yet to be done.
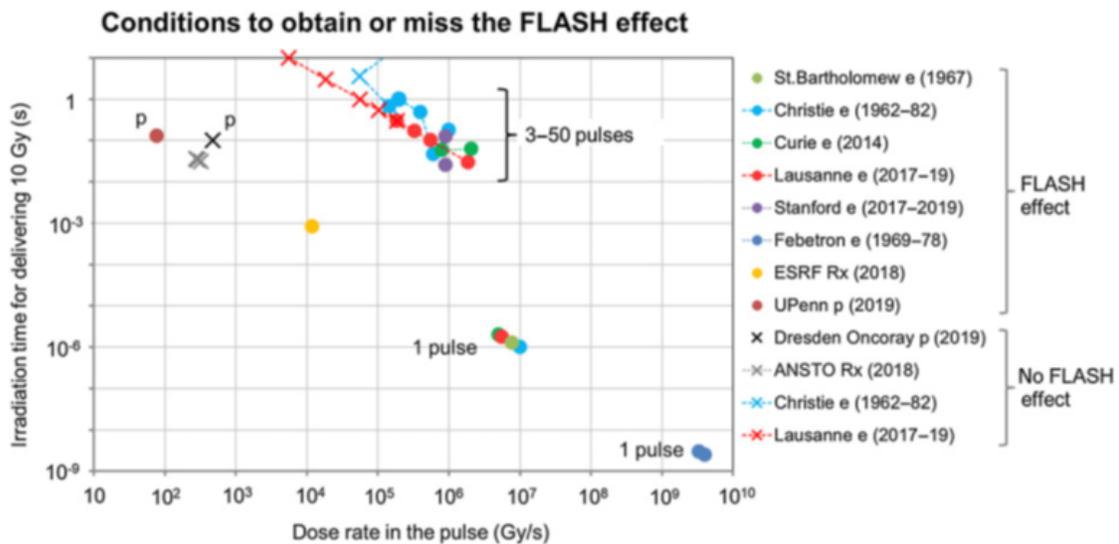
Figure 1. Summary of preclinical studies at different accelerator facilities with different radiation types (right panel). Note the irradiation time for delivering 10 Gy on the vertical axis and the instantaneous dose rate on the horizontal axis. The FLASH effect begins at ~10^5 Gy/sec dose rate during the pulse and a < 1 sec delivery time, where 0.1 s duration and 106/s instantaneous dose rate are firmly in the FLASH region. FLASH effects were seen with nanosecond pulses and more than 10^9 Gy/sec. Reproduced from Montay-Gruel P et al. [8]

2.1 FLASH with electron beams

Highlights of observed FLASH effects from <10 MeV electron beams using 100 Hz clinical linacs are listed below with references. Beam properties from a compilation of studies observing FLASH electron beam conditions are summarized in Table 1.

- Study of pulmonary fibrosis from irradiation of the lung [1]
    - Severe to moderate for conventional average dose rate of 0.03 Gy/sec, 17 Gy total dose
    - For an average dose rate of 40-60 Gy/sec, equivalent fibrosis occurred at 30 Gy total dose
- Study of neurocognitive impairment in mice from brain irradiation [5]
    - Severe neurocognitive degeneration at an average dose rate of 0.1 Gy/sec, 10 Gy total dose
    - Reduced impairment starts at 30 Gy/sec with no neurocognitive decline at 100 Gy/sec average dose rate for 10 Gy!
- Skin irradiation (mini-pig) [6]
    - Fibrosis and necrotic lesions were observed at an average dose rate of 0.08 Gy/sec (22-37 Gy total dose)
    - Only mild depigmentation at an average dose rate of 300 Gy/sec (22-37 total dose)!

Table 1. Preclinical FLASH properties relevant to a clinical application of FLASH

Electron Beam	Min for observed FLASH	Optimal for FLASH
Average Dose Rate	40 Gy/sec	100 Gy/sec
Instantaneous Dose Rate	~10^5 Gy/sec	$\geq 10^6$ Gy/sec

Total Dose	10 Gy	≥10 Gy – tissue dependent
Delivery Time for 10 Gy	nanoseconds	<1 second

Additionally, there are proposals for Very High Energy Electron beams (VHEE) for a more penetrating clinical electron beam. Tumor depths of 30 cm require 200-250 MeV electrons. Treatment models have predicted that to deliver 10 Gy/sec requires 10^{11} e/sec for a 200 MeV, σ=1.5 mm Gaussian beam (D. Bartosik, private communication). Although not discussed in depth here, there are existing electron accelerator facilities that could be used for FLASH studies. The 5Hz FAST SRF Linac at Fermilab produces 50 and 300 MeV beams capable of delivering up to 1000 Gy/pulse and a 10^6 Gy/sec instantaneous rate based on the above simulation. Clinical scanning capability requires a faster duty cycle of ~100 Hz or higher. The CBETA CW recirculating energy recovery linac at Cornell University produces a 150 MeV beam and can scan 10^6 Gy/sec at 200 cm/ms (beyond current transverse scanning capability). The size of the ring can be dramatically reduced by replacing the weak permanent magnets in the arcs, and a miniaturized version is under conceptual design.

2.2 FLASH with photon beams

Photon dose rates produced using clinical electron linacs are too low, and no FLASH effects have been observed. FLASH dose rates can be produced using a high-intensity SRF electron linac with a tungsten target, and a significant FLASH effect was observed for lungs and other tissues. An early 1969 study using high-dose-rate X-rays delivered with nanosecond pulses to mammalian cells in vitro showed sparing effects compared to conventional dose rate [9]. A recent Monte Carlo

Study [10] suggests that FLASH with X-ray tubes may be possible, and a first experimental demonstration of the FLASH effect with X-rays was reported by Gao et al. [11]

High dose rates of photons can also be produced using light-source synchrotrons, notably Synchrotron Broad-Beam Radiation therapy (SBBR) and Microbeam Radiation therapy (MRT) which generates a grid of "pencil" photon beams1. For the SBBR, one study did not show a FLASH effect (37 – 41 Gy/sec, 4-28 Gy) [11]. Still, a second study involving mouse-brain irradiation (37 Gy/sec, 10 Gy) showed significant cognitive sparing similar to the experience with electron FLASH [12]. The main difference between the two studies was that the second had a vertical beam size that was 20 times smaller than the first. The MRT preclinical studies generate a parallel beam array, with 25-100 µm wide peaks and 100-400 µm wide valleys. The peak average dose rate was ~300 Gy/sec, but the valley average dose rate was a lower factor of ~30, and the valleys were a strong indicator of toxicity. The low valley dose rates were conjectured to be the reason for the absence of the FLASH effect.

2.3 FLASH with proton and ion beams

Although pulsed FLASH has been proposed using large synchrotrons and fast extraction, the dose volume remains small and scanning problematic as the beam would likely be re-positioned between spills which makes the treatment time likely incompatible with FLASH conditions. FLASH requires ultra-high repetition rates like the electron linacs or CW beam as output from 230-250 MeV proton therapy iso-cyclotrons. The FLASH effect is only observed with shoot-through (non-degraded) beams that can achieve FLASH intensities. This high-energy beam places the Bragg peak behind the targeted area. To date, there are relatively few proton FLASH studies with mixed results [14,15]. However, many more preclinical studies are underway. Individual RF

(MHz) proton bunch structure may be important for proton FLASH (see Discussion below); proton RF "bunches' are fractions of a microsecond, and electron RF bunches are fractions of a nanosecond. Further, CW proton beams are "quasi-continuous" whereas 100-300 Hz electron linacs produce an ~microsecond "macro-pulse" containing many RF bunches and the "instantaneous" dose rate is averaged over the macro-pulse. For proton FLASH, it can be hypothesized that the instantaneous dose rate of $10^5 - 10^6$ Gy/sec must be achieved across the RF bunch pulse. For pulsed electron beams, the instantaneous dose rate is integrated over the microsecond individual macro-pulse, which repeats at the 100-300 Hz rate of the pulsed clinical linac., as shown in Figure 2. The usually quoted 100 ms treatment time as optimal for FLASH may not apply to quasi-continuous proton beams or CW SRF electron linacs.
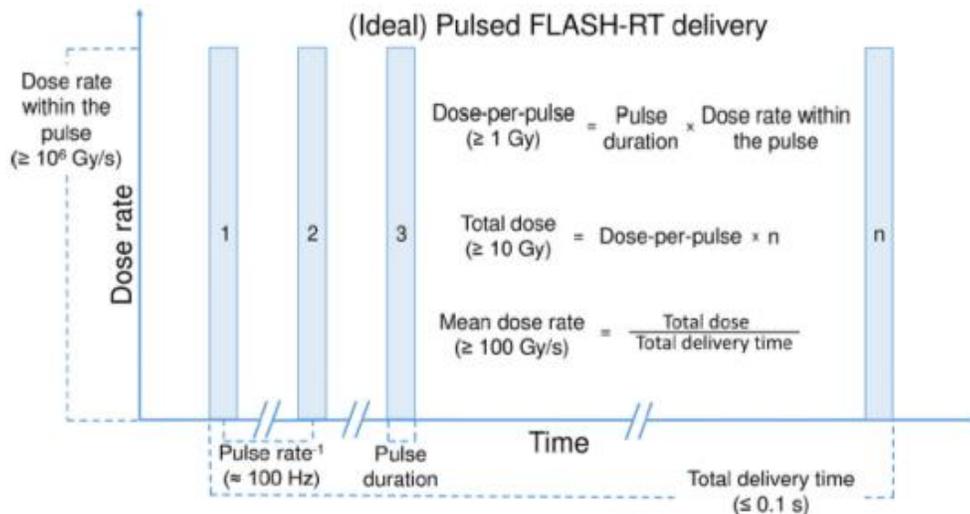
Figure 2. Schematic view of pulsed beam delivery inducing the FLASH effect. Reproduced from Montay-Wilson JD et al. [7]

FLASH intensities have been demonstrated using proton-therapy iso-cyclotrons (cyclotrons that produce continuous rather than pulsed beams) and are currently the only proton facilities capable of participating in FLASH preclinical patient trials. In regard to ion therapy, currently only

synchrotrons are available and synchrotrons, even the rapid cycling 15 Hz ion synchrotron, are not capable of producing the intense ion beams required for FLASH radiotherapy for a clinical application. In addition to providing intense ion beams, FLASH radiotherapy studies need to be extended to incorporate the Bragg peak, range dependencies, and dosimetry into a broader research initiative. Since there are innovative accelerator technologies under development that may provide FLASH intensities for protons and ions, beam conditions can be proposed for the FLASH effect based on RBEs and LETs between the different particle beams. These extrapolations are presented in Table 2 and compared with a more conventional dose rate and fraction.

Table 2. Dose delivery requirements for FLASH for protons and ions extrapolated from electron FLASH studies

Dose Delivery Mode	Protons	Helium	Carbon
Conventional Fraction: 2.6 Gy/fraction Delivery time: 100 sec	2.6×10^9 p/sec 0.4 nA	6.5×10^8 He/sec 0.2 nA	2.2×10^8 C/sec 0.2 nA
FLASH: ≥10 Gy/fraction Delivery Time: 100 msec	1×10^{13} p/sec 1.6 μA	2.5×10^{12} He/sec 0.8 μA	0.8×10^{12} C/sec 0.8 μA

2.4 Discussion

Most preclinical studies published to date have not been systematically coordinated around beam parameters, including mean and instantaneous dose rate, total dose, pulse structure, fractionation, and radiation type. Although there is a wide range of dose rates, some observations can be made nonetheless, although these may apply only to electron FLASH.[5,7,12].

- FLASH effects – general
  - Appear at average dose rates >30 Gy/sec, apparent optimal at 100 Gy/sec
  - FLASH effect likely highly tissue dependent
- Dependence on the beam structure and uniformity in dose deposition
  - Beam delivery
  - Typical dose delivery time for a consistent (electron) FLASH effect is ~100 milliseconds (best <250 ms)
  - MOST positive FLASH studies used a pulsed clinical electron linac with a beam pulse length of ~microseconds and a repetition rate of 100-400 Hz.
  - Instantaneous (within the pulse) minimum FLASH dose rate is 10^6 Gy/sec (again, a characteristic of clinical electron linacs).
- Dosimetry and treatment planning questions
  - Observed volumetric dose deposition dependence
  - Low dose-rate areas not tolerated during FLASH – toxicity reappears2
  - Bragg peak and pencil beam scanning questions: do distal edge and penumbra effects and associated lower-dose rate beam "halos" create a problem?
  - Can a relatively large target volume be uniformly irradiated by fractionated FLASH compatible deliveries over a longer time frame?
  - Instantaneous FLASH dose rate and delivery time for 10 Gy -is it consistent for all radiation types

3 Emerging accelerator technologies for FLASH-RT

3.1 High-gradient ion linacs for FLASH-RT with ion beams

Synchrotrons are used for ion beam therapy, while cyclotrons are mainly used for proton therapy. Until recently, linacs were not seriously considered for ion beam therapy due to the required accelerator length and extended footprint. With the recent developments of high-frequency high-gradient accelerating copper structures, more compact linacs are being proposed for protons and ions. These structures should be capable of delivering FLASH beam intensities.

3.1.1   Linacs for ion beam therapy

Being a single-pass machine, a pulsed linear accelerator (linac) is capable of adjusting the pulse repetition rate and the beam energy hundreds of times per second (~ 200 Hz). This much-desired flexibility in beam tuning enables fast and efficient beam scanning to allow 3D dose painting, as well as real-time image-guided range calculation and targeting of moving targets. By changing the pulse repetition rate, the beam intensity could be adjusted up to 10^9 ions per second (10^{10} for protons), typically needed for therapy. For carbon ions, the energy could be changed continuously up to the full energy of 430 MeV/u required to penetrate the depth of a human body, which is equivalent to 30 cm of water. In addition, the beam quality from a single-pass full energy linac is generally better than other systems that may require energy degraders or multi-turn acceleration.

Linacs have already been proposed for proton [16] and carbon beam therapy [17], but no all-linac-based facilities exist. This is due to the length and space required for the linac, which has limited its deployment in a hospital or other clinical setting. Using traditional accelerator technology, a linac would be hundreds of meters long, and this is the main reason why synchrotrons are currently dominating the field of ion beam therapy. The beam delivery from a linac will be similar to synchrotron beam delivery through fixed beamlines or gantry systems. However, the superior beam quality of the linac enables much smaller magnets and, therefore, more compact gantries.

3.1.2 The ACCIL ion linac: General and FLASH capabilities

The Advanced Compact Carbon Ion Linac (ACCIL) is the most compact full-energy carbon

ion linac proposed for therapy [18]. In Europe, there are proposals for a combined cyclotron and

linac (cyclinac) and an all-linac for carbon beams [19] [not really clear to me how Ref.3.1.2 fits in

here], in addition to the ongoing LIGHT project for a proton therapy linac [19] [same here]. ACCIL

is designed to deliver a full energy of 450 MeV/u, which exceeds the maximum energy required

for carbon ion therapy. It is also capable of accelerating protons and many other ion beams to the

same energy per nucleon. Figure 3 presents a schematic layout of the ACCIL design. The system

is about 45 m long but could, in principle, be folded into two 25 m long sections.
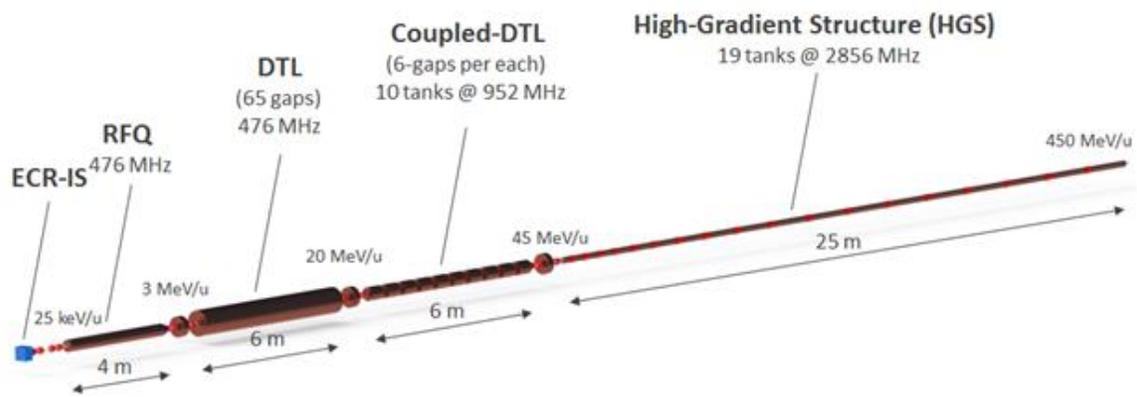
Figure 3. Layout of the proposed ACCIL design.

The linac is comprised of an electron cyclotron resonance ion source, followed by a radio-

frequency quadrupole accelerating the carbon beam to 3 MeV/u, which is further accelerated in a

drift tube linac (DTL), then in a coupled DTL linac up to 45 MeV/u. The essential features to

achieve compactness in the ACCIL design are high-gradient structures, each capable of delivering

50 MV/m, that accelerate the beam to the full energy of 450 MeV/u in ~ 25 meters.

The main advantages of ACCIL are fast pulse-to-pulse beam energy change and ion beam switching capabilities. Different ion sources could be used in the front-end to allow fast beam switching between different ion species. The delivered beam intensity could also be controlled by adjusting the pulse length at the source or changing the pulse repetition rate, typically from 100 to 400 pulses per second (pps) are possible, and R&D for accelerating structures capable of operating at 1000 pps is ongoing. Ultimately, the tuning flexibility of the ACCIL design will allow fast and effective variable-energy and intensity-modulated multi-ion beam therapy.

ACCIL is capable of accelerating a variety of ion beams from proton to neon, up to a maximum energy of 450 MeV/u. At this energy, ions lighter than carbon, including protons and helium ions, have ranges exceeding the depth of the human body and could therefore be used for imaging such as proton tomography. It is also possible to deliver these beams with lower energies for treatment. Despite having ranges shorter than the human body, ions heavier than carbon, like oxygen and neon, could still be used for treatment at adjustable energies up to the full linac energy.

As for FLASH, ACCIL's capability is comparable to other existing proton and ion machines [20]. For example, for a proton beam of 230 MeV, losing about half of its energy in the last 10 cm, the energy deposited at 10^{10} p/s is ~ 0.16 J/s. The corresponding dose delivered to a spot size of ~ 5x5 mm2 (2.5 cm3 beam stopping volume) is 64 Gy/s, which is well above the FLASH dose requirement of 40 Gy/s. For a carbon ion beam of 430 MeV/u, losing about half of its energy in the last 10 cm, the energy deposited at 10^{9} p/s is ~ 0.38 J/s, and the corresponding dose delivered to the same stopping volume is 152 Gy/s, which exceeds the FLASH dose requirement and calls for a larger beam spot size. However, to satisfy all cases, for all tumor sizes and beam energies, we would need at least 10 times more particles per second (10^{11} protons/s and 10^{10} carbon ions/s),

which is feasible with the ACCIL linac design. In addition, higher repetition rates may be required for faster beam scanning and more flexibility in beam delivery.

3.1.2 Enabling technology: Low-velocity high-gradient accelerating structure development

ACCIL requires the development of high-gradient structures (~ 50 MV/m) for ion acceleration with a relative velocity β in the 0.3-0.8 range. This makes the accelerating cells much more compact than $\beta\sim1$ cells built for electrons, especially at the lowest β. A shorter and more compact cell increases the rate of electric breakdowns and makes dissipating the power required for operation at such high gradients challenging. Research and development (R&D) in this field is being pursued at CERN [21], other European institutions, and more recently in the US by Radiabeam and Argonne [22]. In this collaboration, we have developed a $\beta \sim 0.3$ traveling-wave S-band structure (NHS) and demonstrated the 50 MV/m accelerating gradient required for ACCIL [23], see Figure 4. This special cavity design for the lowest velocity ions is what distinguishes ACCIL and makes it more compact than other linacs. It allows the transition to high-gradient acceleration to take place at 45 MeV/u, which is much lower than the 70 MeV/u for other linacs. At Argonne, we have also designed and prototyped a cold model of a $\beta \sim 0.4$ annular coupled structure (ACS) [24] as the next accelerating cavity for ACCIL following the NHS, see Figure 5,
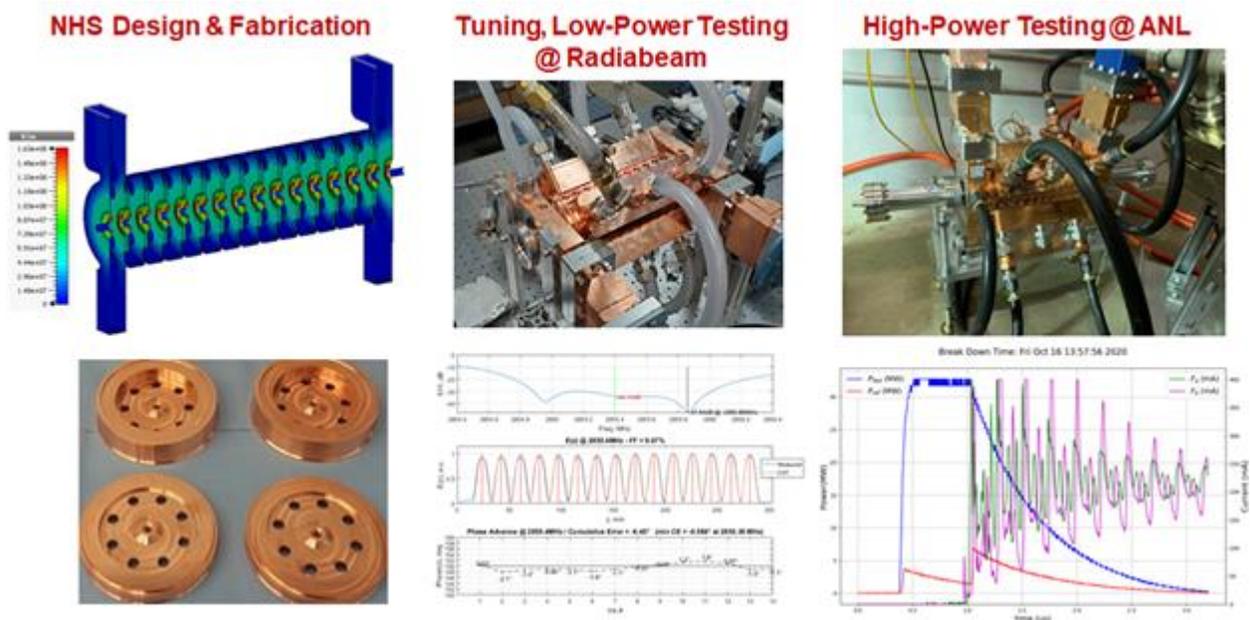
Figure 4. Design, fabrication, and high-power testing of the negative-harmonic traveling-wave structure (NHS) developed by Radiabeam in collaboration with Argonne.
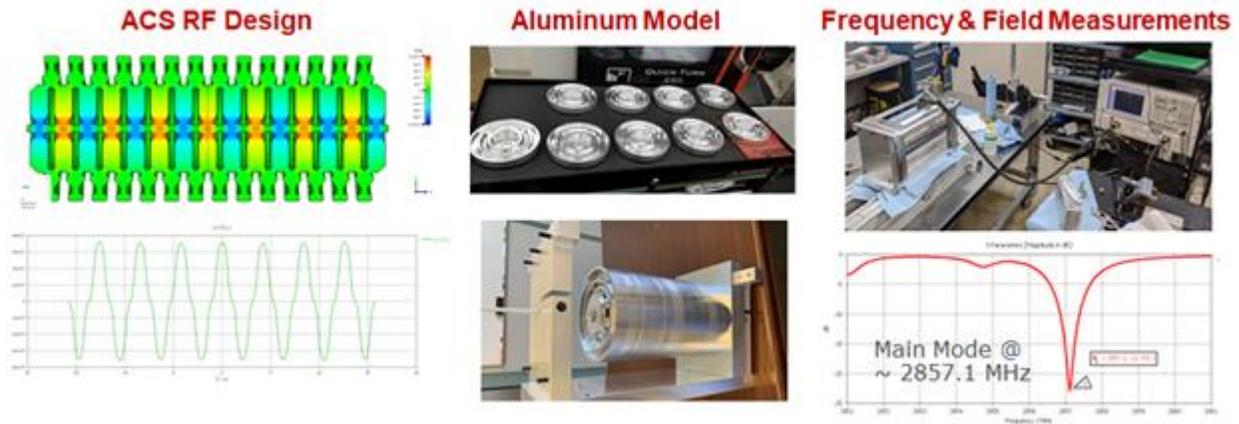
Figure 5. Design, cold model, and measurements of the annular-coupled structure (ACS) developed by Argonne in collaboration with Radiabeam.

3.1.4 Future developments - Path forward

In addition to the general development of high-gradient accelerator structures for low-velocity

ions, we identify a few areas of R&D of special importance for FLASH-RT with ion beams:

- Investigating and pushing the beam current limit of compact ion linacs

- Increasing the repetition rate of high-gradient structures

- Developing RF sources capable of delivering the required high pulsed power

More importantly and to enable this technology, establishing a linac-based advanced ion therapy research center in one of the National Labs would be a significant step forward and would allow the following:

- Cancer therapy and radiobiology research with all ion beams up to neon

- Radiography and tomography with ions lighter than carbon: proton, helium, …

- Real-time MRI guidance during beam delivery, significantly enhancing the outcome of ion beam therapy

- PET imaging using positron emitters (C-11, N-13, O-15, …) produced in the tumor for dose verification

- FLASH ion therapy (FLASH IT) and other novel approaches

We mention, in particular, an ACCIL-type linac that could be installed at the existing IPNS site at Argonne National Lab. with the required infrastructure [25], which represents a significant cost saving compared to a greenfield installation. Following the development and commissioning phases, an initial research program including cellular radiobiology and animal therapy could be conducted prior to human therapy and early clinical trials to prepare for FDA approval.

3.2 Fixed field gradient accelerators for FLASH-RT

3.2.1 Scaling fixed field gradient accelerator

Fixed Field Gradient Accelerators (FFGA), previously called Fixed-Field Alternating Gradient (FFAG) accelerators, are synchro-cyclotron style accelerators based on cycled radio-frequency acceleration. Similar to synchro-cyclotrons, FFAGs generally operate at high repetition rates, e.g., the new superconducting synchro-cyclotron (S2C2) from IBA operates at 1 kHz [26]. Compared to synchro-cyclotrons, a crucial difference of FFGAs is their strong focusing optics (no different from the optical principle of present days' pulsed synchrotrons) which results in much smaller beam size, as well as efficient handling of space charge defocusing effects, a concern when aiming at high charge bunches.

FFGA proton accelerators (aka "scaling FFAG") were developed at KEK in the late 1990s, with a proof-of-principle 500 MeV ring in 1999 [27] and a full-scale 150 MeV ring that provided the first beam in 2005 [28]. Two such rings are in operation in Japan, at Kyushu University (providing beam for condensed matter research) and at the Kyoto University research reactor (providing beam for KUCA, an ADS-Reactor Critical Assembly) [28]. These rings have demonstrated 100 Hz capability based on a single RF system; however, they may even do better as their lattice lends itself to multiple RF systems (in the manner of a folded linac).

Kyoto and Kyushu rings use so-called radial optics, an alternation of positive and negative bend radial sector strong focusing dipoles; compact rings, in addition, are obtained using spiral sector optics. This has been demonstrated by the RACCAM (Recherche en ACCelerateurs pour Applications Medicales) project [29], which has produced a design with a multiple-extraction ring

(Figure 6), RACCAM constructed, as a proof-of-principle, a strong-focusing spiral sector FFGA dipole [30] and validated the design with 3D magnetic field measurements which proved that the expected performance was reached [31].
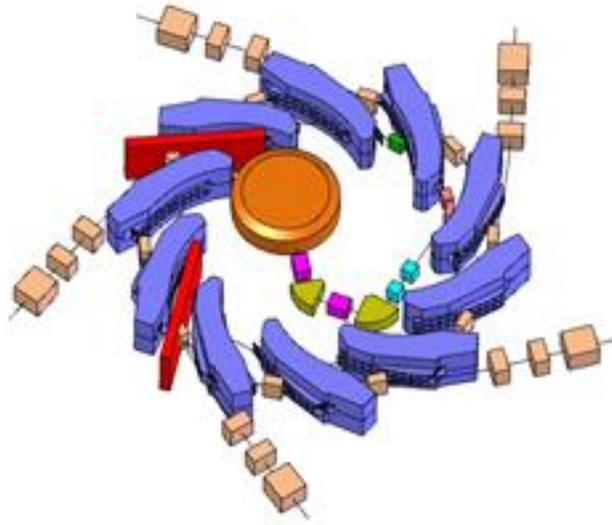
Figure 6. RACCAM multiple-extraction proton therapy FFGA ring [31].

The RACCAM spiral sector ring design allows >5 Gy^{x}liter/min dose delivery, based on bunch-to-voxel delivery. The reference volume (1 liter) is centered at 10 cm depth and comprised of 20^{x}20^{x}20, 5^{x}5^{x}5 mm^3 voxels [29]. This delivery mode requires a total of 10^{11} protons and for a uniform spread out Bragg peak 10^9 protons per bunch in the most distal layer. Thus, the average dose rate is 5 Gy^{x}l/60 s ~ 0.1 Gy/sec over a liter.

The distal layer voxels require 10^9 protons each (by contrast, upstream layers which take the dE/dx of more distal ones require decreasing bunch charge with decreasing depth), thus each 10^9 proton bunch delivers 5 J/8000 ~7e-4 J; bunch length at extraction is~0.1 µs (about half a period of 5 MHz RF), this represents an instantaneous dose of ~7e-4/1e-7=4^{x}10^3 J/s. Thus, regarding

19

FLASH requirements, the average dose rate is by a factor ~200 low, and the instantaneous dose rate by about a factor of 40. Increasing the dose rate could be split between repetition rate, pushing beyond 100 Hz, bunch charge, pushing beyond 10^9 protons per bunch (ppb), and decreasing the irradiated volume. In particular, with the assumption of 100 Hz repetition rate, a required <200 ms irradiation time imposes <40 voxels, 5 ml; current-wise this is $<I> = 10^9$ ppb^{x}e^{x}100 Hz=16 nA. An increase of the repetition rate by a factor of 10, to 1 kHz, would allow irradiation of a 50 ml volume irradiation in 200 ms; it would also bring the necessary bunch charge for proper average and instantaneous dose rates to 4^x10^9 protons; current-wise, this is ~1 μA.

It can be seen from what precedes that increasing the average current (via repetition rate and/or bunch charge) and instantaneous current (via bunch charge) towards FLASH requirements is challenging. An intermediate option is to consider a smaller working volume, 10s of ml, for instance, which would relax on repetition rate and bunch charge constraints.

3.2.2 Nonscaling FFGA for FLASH

The constraints imposed by the field scaling law are relaxed in the nonscaling variant of the FFGA. Advanced codes and optimizers have been used to stabilize the machine tune consistent with isochronous orbits as in an iso-cyclotron. Isochronous orbits permit CW, high intensity beam, and the strong-focusing gradients allow long straight sections like a synchrotron. These straights can be used for high-gradient acceleration and low-loss, variable energy extraction using large-aperture bump magnets. The system design applied to therapy is described below.

Overview

A compact 250 MeV/nucleon, fixed-magnetic field turnkey machine has been designed in a racetrack format with variable energy continuous-output beam without a degrader, and with low-loss operation. The design is isochronous and produces continuous beam for ion species with a charge to mass ratio of ½ (H_2^+, D^+, He^{2+}, Li^{3+}, B^{5+}, C^{6+}, N^{7+}, O^{8+}, Ne^{10+}) and is therefore capable of accelerating all ion species to therapeutic energies. An outer ring can be added to further the energy reach of the ions to the full 430 MeV/nucleon.

Accelerating ions with an approximately constant charge to mass ratio has the advantage of equal beam transmission independent of ion species. Identical operation and extraction are maintained for all the therapeutic ions, including protons (H_2^+), implying turnkey operation even when switching between ions. Further, the possibility of accelerating and extracting multi-ion composite beams from a mix, or cocktail, of injected ion species (with an effectively equivalent charge to mass ratio) is ground-breaking technology. This approach also provides rapid switching between ion species, a capability based on <1% rapid adjustments in the RF frequency.

The complete system involves the injector, a preaccelerator, and the therapy ring – similar to cascade synchrotron systems. To allow variable energy extraction in a long straight section, the energy range must be restricted in order to extract inner, low-energy orbits using extraction magnets with feasible strengths and, in particular, apertures. The preaccelerator extraction energy not only facilitates variable-energy extraction in the higher energy ring but can also support an independent beamline for eye treatments and R&D.

The High-Energy Therapeutic Ring

The high-energy ring will be operated from 100 MeV/nucleon up to 250/330 MeV/nucleon to support ion therapy and particle imaging. This energy represents a 15 cm range for carbon and the energy required for light-ion imaging for pelvic or abdominal scans. The design of the therapeutic ring is a racetrack with opposing 5 m straight sections for RF and injection/extraction (2-fold periodicity). The ring also incorporates a 2m short straight in the center of each arc for vacuum and diagnostics. Figure 7 shows the layout of the ring and relative size compared to the Heidelberg Ion Therapy facility, which is a slow-cycling synchrotron capable of 430 MeV/nucleon. Particle tracking has been performed and has a large dynamic aperture with an acceptance>1000 mm-mr (normalized). Arcs can be either SC or normal conducting. SC extends the energy reach of the extraction system due to a reduced aperture and smaller distance between circulating orbits. However, the orbit separation needs to be studied and optimized for efficient and clean extraction of different energy orbits and the required acceleration gradient. An acceleration of ~2MeV/turn per nucleon appears to be a maximum step size requirement for longitudinal scanning. The isochronous level of performance in machine design shows less than a percent variation in TOF over an acceleration range from 70 MeV/nucleon to 250 MeV/nucleon.
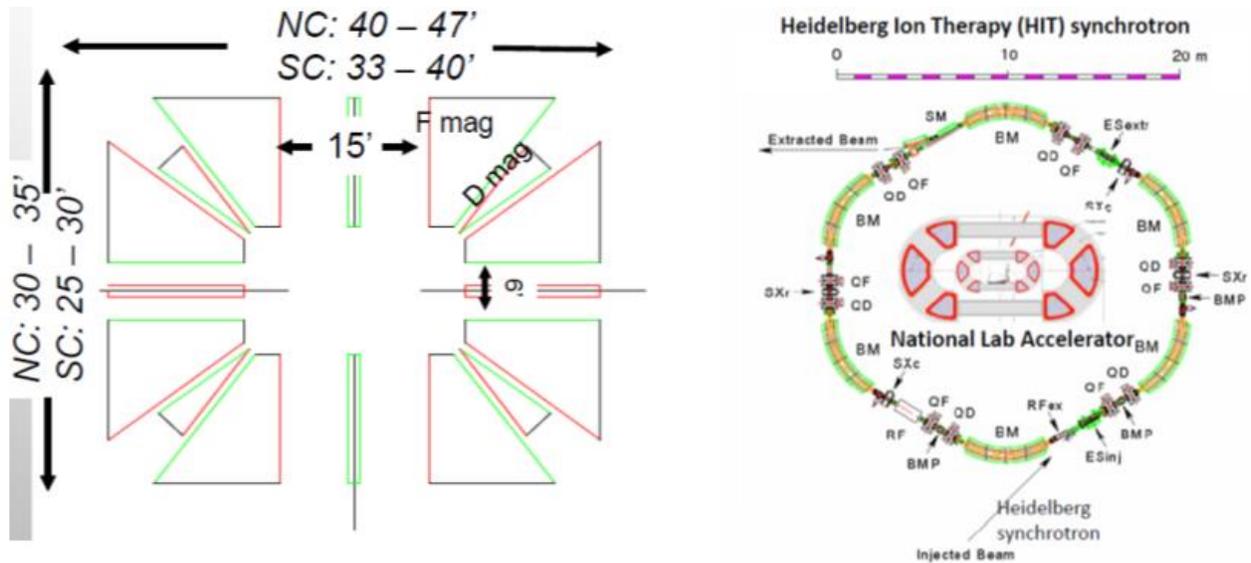
Figure 7. Outer dimensions for a variable energy 330 MeV/nucleon therapeutic ring (left) and a dual ring system 430 MeV/nucleon (right) compared with the Heidelberg Ion Therapy facility. On the right, the FLASH-capable, CW and variable-energy 430-MeV/nucleon ion accelerator nested system is compared to equivalent-energy, low-duty cycle Heidelberg Ion therapy Synchrotron. Inner ring racetrack is 250 MeV/nucleon and can provide independent beam delivery.

Variable energy extraction

Extraction is performed in one of the 5 m straight sections and shown in Figure 8. The magnets can be ramped for swept, variable energy longitudinal scanning or set at a flat-top for single energy beam delivery. The field direction is bipolar; field decreases and flips sign for maximum inner orbit extraction (blue to red lines). Extraction magnetic fields are limited to ~2.5T for a ramped system.
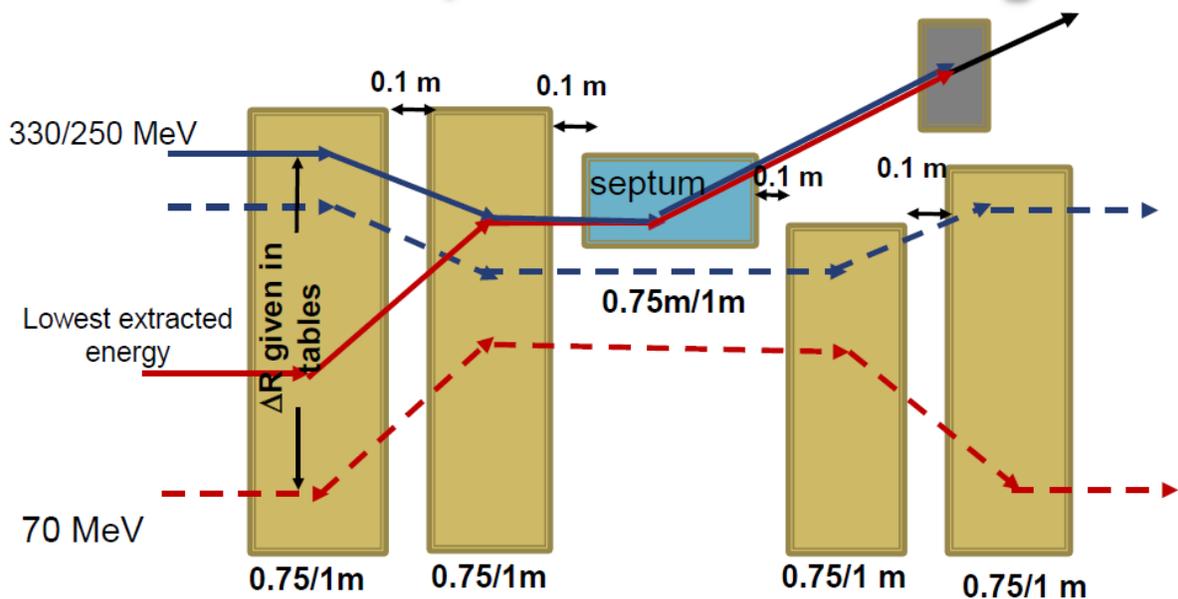
Figure 8. Layout of the ramped, bipolar magnet extraction system that selects the orbit and energy for extraction through a septum (left). Inner, lower-energy orbits are returned to their respective closed orbits for continued acceleration.

Source, LEBT, RFQ, and Injector

The ion source and beam capture system are comprised of an Electron-Cyclotron-Resonance (ECR) source coupled to a Radio-Frequency Quadrupole linac (RFQ) through a conventional Low-Energy Beam Transport (LEBT) section, as shown in Figure 9. The ion ECR source has one of the highest ionization efficiencies for gaseous elements. An RFQ linac, which uses electrical RF focusing, can capture, auto-bunch, and efficiently accelerate DC (constant current) ion beams directly from the source, achieving energies of several MeV, efficiently replacing complex and lengthy pre-injector elements. The LEBT will consist of an Einzel and solenoid lens system (beam chopping may be required to match RF frequencies between RFQ and injector). In addition, a mixture of ion species can be ionized in ECRs to produce a mixed or 'cocktail' of ion beams which potentially can be accelerated in the proposed accelerator system – including all therapeutic ions

plus protons in the form of H_2^+ – thus combining imaging and therapeutic beams for real-time dosimetry.

An advanced, small-footprint, heavy-ion injector iso-cyclotron has been developed for the injector. This novel normal conducting, separated-sector injector has an optimized strong-focusing field gradient designed to efficiently accelerate light ions with a charge-to-mass near ½ (namely, protons in the form of H_2^+, D^+, He^{2+}, Li^{3+}, B^{5+}, C^{6+}, N^{7+}, O^{8+}, Ne^{10+}, $S^{16+,}$ and Ca^{20+}) scalable up to 70 - 100 MeV/u [32,33]. Dual, high-gradient, 0.2 MV cavities with a tuning range of ±1% in frequency can accelerate any ion species with this charge to mass ratio on the 8th harmonic (~45 MHz) with large turn-to-turn, almost centimeter-level separation; an enabling compact and low-loss extraction technology that eliminates the charge-changing foils (used for injection in ion synchrotrons and extraction in H^- cyclotrons). Low (percent level or less) extraction losses are projected to be compared with the 20% - 60% (or even higher) losses of proton-therapy CW cyclotrons at extraction.
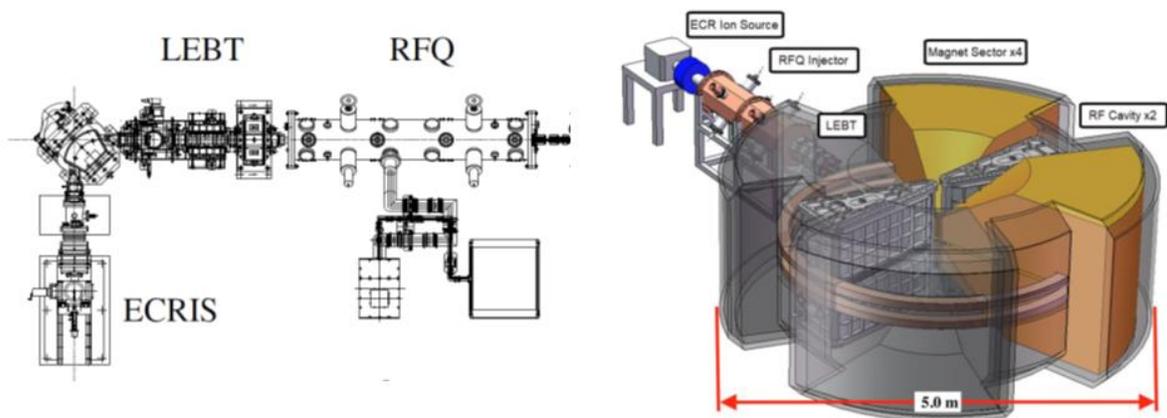
Figure 9. HIMAC, Japan ion source and RFQ (left), which serves as the concept for the upstream pre-acceleration system for the injector accelerator (right)A CAD model of the full conceptual design of the 20 MeV/u injector system (scalable to 70-100 MeV/nucleon) is shown on the right. From left to right, the ECR ion source, focusing solenoid, RFQ, beam focusing quadrupoles, and the cyclotron are shown with a transparent outer shielding for clarity.

Summary

A complete CW, variable-energy ion therapy concept has been developed with the preaccelerator stage design advanced in terms of engineering. Since FLASH intensities have been achieved and the effect observed using proton iso-cyclotrons, this ion therapy complex is FLASH capable. Further, it has the advantage of supporting essential R&D beyond the shoot-through beams currently available for hadron R&D. In addition to providing intense ion beams, FLASH radiotherapy studies can be extended to incorporate the Bragg peak range dependencies and dosimetry into a broader research initiative. The injector and higher-energy therapy accelerator being developed for the National Particle Beam Therapy Center (Waco, TX) will provide the range of ions intensities with different LET and relative biological effectiveness (RBE) requested by the medical community in a CW beam format without significant operational modifications and overhead; i.e., a turnkey system. This system represents a significant advance in ion therapy clinical application and plays a critical role in the development of FLASH-RT.

3.3 FLASH studies with laser-driven particle sources

3.3.1 Status of laser-driven particle sources

Novel laser-driven particle sources are receiving increasing attention due to their potential of providing particle beams for applications on a relatively small footprint and at a potentially lower cost than radiofrequency (RF) driven accelerators [34,35]. Efficient laser-particle acceleration has become feasible with the advent of ultra-short pulse high-power lasers enabled by chirped pulse amplification [36], a technology that was awarded the Nobel Prize in Physics in 2018, which yielded peak laser powers exceeding 1 petawatt (PW) [37]. The most prominent acceleration schemes are laser wakefield acceleration (LWFA) of electrons [38] and target normal sheath

acceleration (TNSA) of protons and ions [39]. LWFA is conducted with gas targets that are quickly ionized by the leading laser pulse edge, followed by the formation of collective plasma oscillations in the wake of the pulse as it propagates through the transparent plasma. Free electrons are accelerated up to several GeV energies in dynamic electric fields associated with the resulting plasma wave [40,41]. If optimized, monoenergetic electron bunches with nC charge can be generated [42]. At the time of writing, Lawrence Berkeley National Laboratory held the LWFA electron energy record, with 8 GeV and a few pC charge [43]. LWFA sources can be used to drive compact light sources from the high-field THz [44] over the high-brightness X-ray [45] to the gamma ray range [46].

Target normal sheath acceleration (TNSA) is generally pursued with solid targets, most commonly in the form of a few μm thick metal or plastic foils. Equally ionized by the lead edge of the laser pulse, the laser peak intensity interacts with free electrons in a preformed plasma layer at the target surface. Electrons gain energy in the laser field, circulate through the target bulk and expand beyond the predominantly fixed ion distribution at the target surfaces. The resulting quasi-static charge separation fields are in the order of TV/m and lead to the acceleration of protons and ions to >10 MeV energies, emitted along the target normal with a beam divergence of roughly $\pm$ 20° [47,48]. The generated proton beams are of high flux (up to 10^{13} particles per pulse [49]) and feature broad exponential energy spectra up to the characteristic cutoff energy, approaching 100 MeV [50-53].

At current PW laser pulse repetition rates of at most 1-10 Hz, directing laser-driven (LD) particle beams to biological samples results in a moderate *mean* dose rate. However, due to their generation mechanism, resulting in ultra-short particle pulse lengths of less than a picosecond at

the source, LD particle beams naturally feature ultra-high *instantaneous* dose rates (IDR), exceeding 10^9 Gy/s. This IDR is several orders of magnitude higher than dose rates typically delivered with RF driven accelerator technology [54].

3.3.2   Using laser-driven particle sources for preclinical radiobiological studies of the FLASH effect

LD particle sources may soon become adequate complements to RF driven accelerators for basic radiobiological research of the FLASH effect [55]. Access to conventional experimental and medical machines has been rather limited for this type of research [56], while the steady increase in available compact LD particle sources has already started to open up new experimental options for systematic radiobiological studies.

The majority of radiobiological studies with LD particle sources has been conducted in view of potential future applications in radiotherapy, in particular with protons and heavier ions. As such, an appreciable number of *in vitro* studies have been conducted to investigate the radiobiological effectiveness of LD protons [57-68]. Fewer radiobiological studies were so far conducted with LD electrons [69-74]. The only *in vivo* study found no difference in tumor growth delay comparing LD electrons and RF accelerated electrons [71]. The proposal of using very high energy electrons (VHEE) with energies in the range of 150 - 250 MeV for radiotherapy [75] has sparked renewed interest in the dosimetric properties and the potential for new radiotherapy protocols using compact LWFA electron sources [76-78]. So far, no differential sparing effect of normal tissue was reported from radiobiological studies with LWFA electrons.

While the dose rate was not always specified in publications, it can be assumed that samples were irradiated at ultra-high IDR due to the LD particle acceleration mechanisms, as mentioned above. So far, the majority of radiobiological studies with LD particle beams were conducted using *in vitro* cell cultures and at atmospheric ~ 20% oxygen levels.

Magnetic transport beamlines have been implemented at a few laser facilities to transport LD protons to a dedicated sample site and apply a three-dimensional dose profile for *in vivo* studies with small animals, for which tumor models have been developed [79-82].
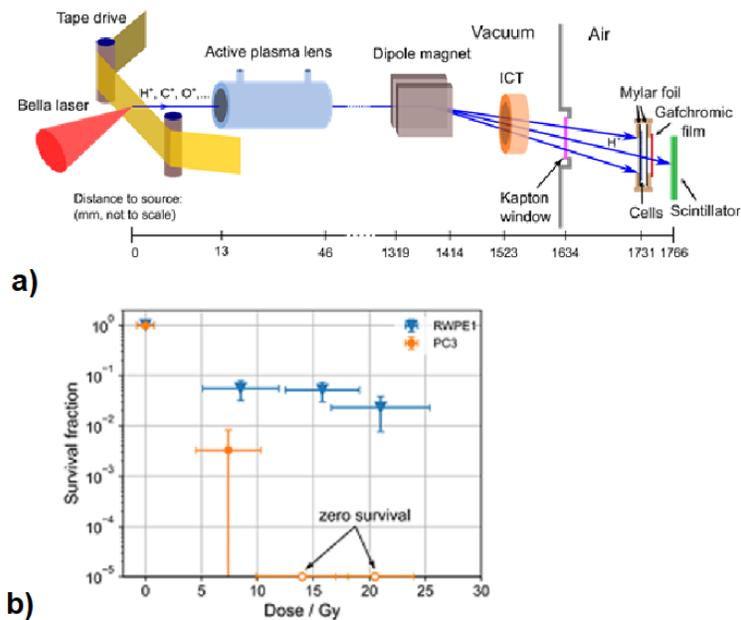
Figure 10. Figure adapted from Ref. [68]. a) Schematic depiction of the laser-driven proton beamline at the BELLA PW laser with tape drive target, active plasma lens, dipole magnet, integrating current transformer (ICT), cell sample, gafchromic film, and scintillator. b) Cell survival fraction of human prostate cancer cells (PC3) and normal human prostate cells (RWPE1) after irradiation with laser-driven protons. c) Proton beam parameters for cell sample irradiations at the BELLA PW

Table 3. Proton beam parameters for cell sample irradiations at the BELLA PW

Dose per pulse	1 Gy
Pulse length	30 ns
Pulse repetition rate	0.2 Hz
Instantaneous dose rate	3×10^7 Gy/s
Mean dose rate	0.2 Gy/s

In a preliminary study at the 40 Joule BELLA petawatt laser proton beamline, it was demonstrated for the first time that LD protons delivered at ultra-high IDR can indeed induce the differential sparing of normal versus tumor cells *in vitro* for total doses ≥ 7 Gy [68]. In that study, normal and tumor prostate cells in 1 cm diameter custom cell cartridges were irradiated with LD protons of 2-8 MeV at an IDR of 10^7 Gy/s. After acceleration from a tape drive target, the proton bunch was transported with a compact active plasma lens beamline [83] to the cell sample site located outside the vacuum chamber (Figure 10 a). An integrating current transformer (ICT) was implemented for online beam charge measurements. The dosimetry was performed with calibrated radiochromic films attached to every cell sample. With 1 Gy applied per laser shot, total dose values up to > 30 Gy were accumulated by operating the LD proton beamline at 0.2 Hz. A significant sparing of normal prostate cells compared to prostate tumor cells was observed after irradiation with LD protons (Figure 10 b). The main proton beam parameters for this study are summarized in Figure 10 c. Reference irradiations with X-rays at clinical dose rates did not show a similarly differential radiosensitivity. It should be pointed out that the generation of LD proton

beams in the energy range sufficient for this type of study does not require a PW laser system but was demonstrated in numerous experiments at 100 TW-class laser systems [52,53].

3.3.3   Potential of laser-driven particle sources for FLASH Radiation Therapy

Preliminary *in vitro* experiments with LD ion sources have shown promise for FLASH radiotherapy [68]. However, stringent requirements concerning combined key beam parameters like proton energy (up to 250 MeV), numbers of protons per bunch (10^9), stability and control of energy and proton numbers from shot to shot (< few percent), and repetition rate (> 10 Hz) are yet to be experimentally demonstrated [84].

Currently, the primary challenge for the field of laser-ion acceleration is reaching clinically relevant particle energies. So far, peak LD proton energies achieved in experiments are approaching 100 MeV [50], which is well below energies necessary for clinically relevant penetration depths of >30 cm in humans [85]. Ongoing efforts to develop a high-repetition rate, several PW-class lasers can theoretically overcome this challenge when combined with improved gantry designs and treatment planning strategies specific to LD particle sources [86,87]. Currently, no unified reference dosimetry protocol exists for LD particle beams, which are unique in their ultra-high IDR and, in the case of ions, broad energy spectra. However, innovative dosimetry methods for radiobiological studies with LD proton sources have been developed that use online, minimally invasive, relative dose detectors, e.g., thin transmission ionization chambers, corrected for recombination effects [88] and cross-referenced with independent absolute dosimetry methods like radiochromic films [89] or Faraday cups [90]. These have enabled *in situ* dose-controlled LD proton irradiations of biological cell samples at a relative dose uncertainty below 10% [91].

Advances in laser technology are expected to deliver higher LD proton and ion energies because experiments and simulations have shown a consistent increase of maximum particle energies with laser pulse energy, power, or intensity [52,53]. At the same time, theory and simulations predict higher proton and ion energies when harnessing advanced acceleration regimes, including, for example, radiation pressure acceleration [92], magnetic vortex acceleration [93], and shock acceleration [94].

Given that the aforementioned ion source requirements are met, designing a hypothetical compact LD FLASH radiotherapy machine requires careful consideration of not only the laser particle source but also the treatment beam delivery system that needs to reliably shape a 6-dimensional dose profile matching the tumor profile of which first designs exist [86]. As such, even after optimizing LD particle sources for footprint, which on the laser side may come naturally with advances in laser technology, it remains to be seen whether they can compete in compactness and cost with emerging conventional proton therapy machines, e.g., compact solutions by Mevion, IBA, Hitachi, and others, which have seen significant developments in recent years to reduce their footprint and cost [84]. However, these machines are typically not able to deliver comparable IDR as LD proton sources. So far, no such compact machines exist for heavier ions, which are automatically accelerated alongside protons in LD ion accelerators.

With the current interest in using VHEE for radiotherapy, LWFA may well offer the most promising method for compact and affordable VHEE medical machines that can operate in the ultra-high IDR regime [35]. While the necessary electron energies are readily generated in a well-controlled laboratory setting, the long-term source stability and reproducibility require further improvement. Moreover, current limitations to the achievable mean dose rate due to lower

repetition rates compared to RF driven accelerators, in combination with a lower, less localized energy deposition compared to ions, need to be addressed. Current efforts towards high average power, Joule-class kHz laser systems may provide solutions for some of these issues [95].

3.3.4 Summary

To summarize, current LD particle source parameters are well below the requirements for their use as an alternative medical FLASH radiotherapy modality. However, their comparatively low-cost and compact nature has earned LD particle sources increasing attention and the differential normal tissue sparing *in vitro* under LD proton irradiation was recently demonstrated [68]. Therefore, LD particle sources could soon complement conventional accelerators to increase and democratize access to particle sources for preclinical radiobiological research. This real-world application can serve as a stepping stone to further advance LD particle sources to the necessary capabilities to provide particle beams for FLASH radiotherapy.

3.4. High peak current linear induction accelerator (LIA) for FLASH-RT[1]

3.4.1 Introduction

Meeting the requirements for reproducible FLASH effects of $>1.8 \times 10^5$ Gy-s^{-1} instantaneous dose rates with an overall irradiation time <200 ms (>40 Gy-s^{-1} average dose rate for healthy tissue sparing) using deep penetrating MV bremsstrahlung (i.e., X-rays) requires tens of ampere pulsed electron beams at high pulse repetition frequency (PRF) [2,96]. These dose rate criteria must not

---

[1] Patents Pending

only be met in the core of the irradiated volume but in the whole of the volume as well (i.e., periphery and exit edge) [12].

The pulsed power based linear induction accelerator (LIA) using a multilayered bremsstrahlung conversion target meets these demanding requirements. Complementary irradiation sources from the same accelerator structure ensure that the whole of the irradiated volume is above the FLASH threshold. The LIA acceleration technique stores energy during the interpulse time and then discharges it in a short, 10s of nanosecond pulse to achieve extremely high instantaneous dose rates. This method is a direct acceleration technique using *induction* and does not require RF or microwave generation as an intermediate step. When operated at a clinician-specified kilohertz PRF, equivalent dose rates exceeding the healthy tissue sparing thresholds can be easily achieved, and the concentration of specific radicals, thought to play a role in the FLASH process, can be manipulated (see for instance [97]). Using active control of the individual pulses ensures safe dosing. While not widely known to the medical community, existing systems have been used as 10s of MeV, kiloampere electron or ampere level hadron sources since the 1960s [98].

A key demonstrated capability of the technology is that the beam pipe can be made arbitrarily large without affecting the acceleration gradient [99,100]. This property enables independently controllable multibeam acceleration through a single accelerator structure for complimentary irradiation. While the gradient of older induction linacs is low (<1 MV/m for 50-70 ns pulses), modern approaches enable 5-10 MV/m gradients. Thus, a 16 MeV system with 4-8 or more individual beams with variable energy and pulse rate would fit in a clinic-sized vault of $\sim$100 m^3.

Figure 11 depicts an artist's conception of a four beam system; added beams are easily implemented [101]. The accelerator cells can be seen beyond the patient and patient couch. Four separate electron beams are being accelerated away from the patient, captured, and then bent 180° with two 90° dipoles. Solenoid transport is then used to return the beam alongside the patient, and a third 90° dipole directs the beam to a target where it is converted to bremsstrahlung. Multi-leaf collimators (MLC) can be used in this region for conformal therapy
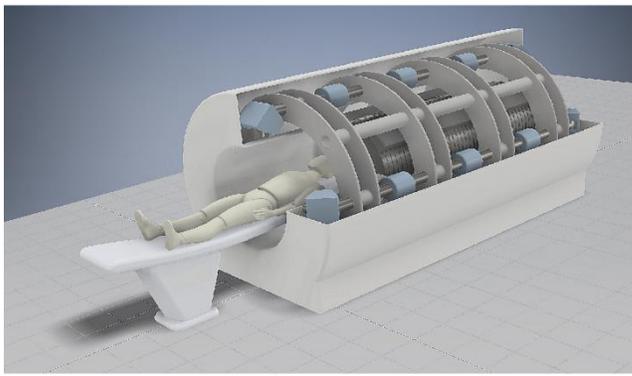
Parameter	Induction Linear Accelerator
Electron Energy (MeV)	16
Total Beam Current (A)	25
Pulse Width (s)	1.50E-08
Pulse Repetition Frequency (Hz)	10000
Net Gradient (MeV/m)	5.0
Accelerator Length (m)	3.20
Inner Radius (cm)	10.0
Instantaneous Surface Dose Rate (Gy/s)	6.60E+05
Average Surface Dose Rate (Gy/s)	98.9
Total Dose (Gy)	19.8
Time On (s)	0.20

Figure 11. Concept FLASH-RT system using a linear induction accelerator (LIA) providing four or more lines-of-sight. LIA is on axis with the patient. Blue components are the magnetic focusing elements that direct the electron beam to the patient. The active accelerator is 3.2 m. With the returning drift section, the overall system length is 3.5 m less the patient couch [101].

3.4.2 Illustrative measurements from LIAs for FLASH-RT

Bremsstrahlung generated by an LIA provides broad area, deep penetrating, and high dose rate capability. This unique capability results from the elimination of resonant structures characteristic of the majority of acceleration techniques. Such structures are prone to pulse shortening beam instabilities and also degradation of the acceleration gradient when beam currents approach one ampere [102-104]. We present measurements on the FLASH X-ray (FXR) accelerator used to accelerate electrons to 17 MeV and briefly describe the Experimental Test Accelerator-II (ETA-II) with a nominal output energy of 6.5 MeV but at kilohertz PRF [105 -107].
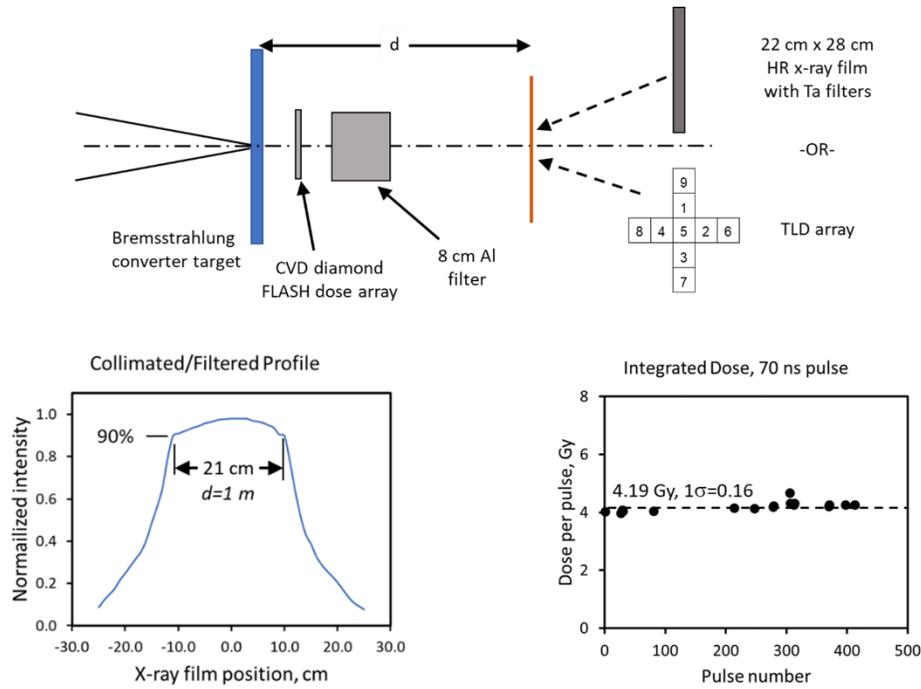
Figure 12. Measurement geometry, bremsstrahlung field flatness, and pulse-to-pulse repeatability.

The FXR geometry and measurements are shown in Figure 12. This particular FXR arrangement consisted of the bremsstrahlung converter target, a fast CVD diamond FLASH dose detector, an 8 cm thick low energy filter, and either thermoluminescent (TLD) or film detector at 1-2 m [107]. The 90-100% flat field is approximately 21 cm diameter at 1 m. This measurement corresponds to an approximately 350 cm^2 area demonstrating that FLASH levels can be maintained in the totality of an irradiated volume. We observe a *single shot, stable* dose of approximately 4.19 Gy with $1\sigma \approx 0.16$ or a 3.9% variation. This value corresponds to an instantaneous dose rate of approximately 6×10^7 Gy-s^{-1}.

On ETA-II, a 5 kHz PRF has been demonstrated. This system also produced highly stable electron beams with less than 1% energy variation, millimeter spot size, and submillimeter spot

motion. Initial use of the accelerator was in conjunction with a wiggler to generate electromagnetic energy at 2 GW and 140 GHz mm-wave energy for fusion research studies [108].

3.3.5   Meeting the criteria for FLASH-RT

To ensure that both the periphery and exit dose rate were above the healthy tissue sparing threshold to minimize toxicity, we performed calculations assuming a minimum of four separate sources placed symmetrically around a water phantom volume approximating the average human torso 16 cm radius [12,109]. Each source provides 25 Gy-s^{-1} at 1 m using a total beam current of 25 A; details are provided elsewhere [101]. This configuration achieved 50% beyond the required average healthy tissue sparing dose rate, or about 60 Gy-s^{-1} throughout most of the volume. By contrast, a single source at the same level achieved the healthy tissue sparing dose rate >40 Gy-s^{-1} nearest the source, but about 25% of the volume is below that dose rate, potentially inducing toxicity. Noting that the total beam current for LIAs typically exceeds 1 kA, current can be used as a free parameter for increased dose rate.

The model assumed a single LIA to accelerate separate beamlets in an approximately 14 cm diameter beam pipe. While four beams are shown, eight or more can be easily implemented in an actual system. Beam transport is managed through the accelerator with solenoid coils and integrated steering similar to the FXR geometry [105]. The added steering capability allows generating oblique rays to allow a closer approximation of multibeam conformal therapy. Based on the model, at 16 MeV, the system would be approximately 3.2 m long (Figure 11), delivering a uniform average dose rate of 60 Gy-s^{-1} at a beam current of 25 A at 10 kHz PRF.

3.5 High-current electron linear accelerator for X-ray FLASH radiation therapy

3.5.1 X-ray FLASH-RT

An attractive tool for delivering FLASH-RT could be a FLASH-capable X-ray system. More than 80% of all radiotherapy is delivered with X-rays [110]. They are the most versatile form of radiation therapy and the most cost effective. Unfortunately, the physical process for generating X-rays is not very efficient [111]; therefore, a high-power accelerator is needed for X-ray FLASH-RT. Furthermore, one would still like to achieve as much conformality as possible. Conformality, combined with the healthy-tissue-sparing FLASH effect, promises to dramatically improve patient outcomes [112].

Considering the inevitable reduction in effective dose rate with intensity modulation and transmission through small apertures, a linac that can deliver 100 Gy in one second or faster is challenging but not impossible. Conventional 6 MV medical linacs produce a flattening filter free dose rate of around 0.2 Gy/s at one meter from the X-ray target – three orders of magnitude too low – however, they are on the low end of the spectrum of linac powers [113]. A typical medical linac has a beam power on the order of 1 kW. In comparison, industrial accelerators for sterilizing food and medical products can achieve beam powers of several hundred kW [114].

Another factor that allows for improvement in dose rate is increasing the beam energy. The conversion efficiency from electron beam power to X-ray power scales approximately with E^3, so a small increase in energy can make a big difference in X-ray intensity. The higher X-ray energy also allows greater penetration. However, there are two major downsides to higher photon energies: larger lateral penumbra (a measure of the fuzziness at the edge of the beam) and greater neutron production (which causes activation and unwanted dose to the patient and the environment). Photon energies up to 20 MV are commonly used in RT. We consider 10-18 MV to be optimal for achieving a high dose rate while limiting the negative factors.

One could also consider reducing the distance from the source to the target. However, this can only be done to a certain point without sacrificing useability. Achieving good conformality requires placing one or more collimators between the beam source and the patient. Along with pure physical limitations on fitting the equipment around the patient, this limits the source-to-surface distance (SSD) to 80 cm at the smallest.

3.5.2 New technology for X-ray FLASH-RT

RadiaBeam and UCLA are working on a solution for X-ray FLASH therapy that takes advantage of a single linac based on already-demonstrated technology and an innovative yet straightforward method for intensity modulation [115]. The major innovation of the proposed project is the development of the Rotational direct Aperture optimization with a Decoupled (ROAD) multi-leaf collimator (MLC) ring [116]. Intensity modulation has been the key driver in improved patient outcomes in RT over the past three decades, but there has been no solution to do this in the short time required by FLASH. With ROAD, the linac pulses are timed to align with a counter-rotating ring of 75 pre-shaped MLC apertures. As both the linac and MLC ring rotate in opposite directions at 60 rpm, 150 modulated beams are delivered in 1 s, each delivering up to 0.7 Gy to the tumor. ROAD can achieve physical dose conformality superior to state-of-the-art VMAT plans free from the MLC mechanical limitation, yet with the added benefit of the FLASH effect. Figure 13 shows a model of the proposed ROAD-FLASH system [13].

The linac (see Table 1 for a summary of parameters) consists of a 1.3 A, 140 kV electron gun, prebuncher, chopper, and two traveling wave linac sections powered by a commercially available 20 MW L-band klystron with 167 µs pulses at 150 Hz, to bring an 8.14 mA average current electron beam to 18 MeV. Assuming a dose conversion factor of 2,000 Gy/min/mA at 18 MeV, such a linac will be able to provide an uncollimated dose rate of 271 Gy/s at 1 m (8.14 mA $\times$ 2 $\cdot$ 10^3/60 Gy/s/mA), which is equivalent to ~100 Gy/s collimated dose at 80 cm, assuming ~25% dose delivery efficiency. The beam is transported through a rotary vacuum joint into a rotating magnetic gantry that brings the beam to a rotating X-ray target directed at the patient.

Table 3. Parameters of ROAD high-current electron linear accelerator for X-ray FLASH therapy

System	ROAD	Conventional [10]
Energy [MeV]	18	6
Pulse Length [μs]	167	4
Rep Rate [Hz]	150	250
Duty Cycle	2.5%	0.1%
Injected current [A]	1.3	0.5
Transmission	25%	25%
Peak current [A]	0.325	0.125
Average Current [mA]	8.14	0.125
Dose Rate Factor [Gy/min/mA at 1 m]	2,000	120
dose rate, uncollimated, at 1 m [Gy/s]	**271**	**0.25**
Dose Delivery Efficiency	25%	25%
dose rate, collimated, at 80 cm SAD [Gy/s]	**106.0**	**0.10**
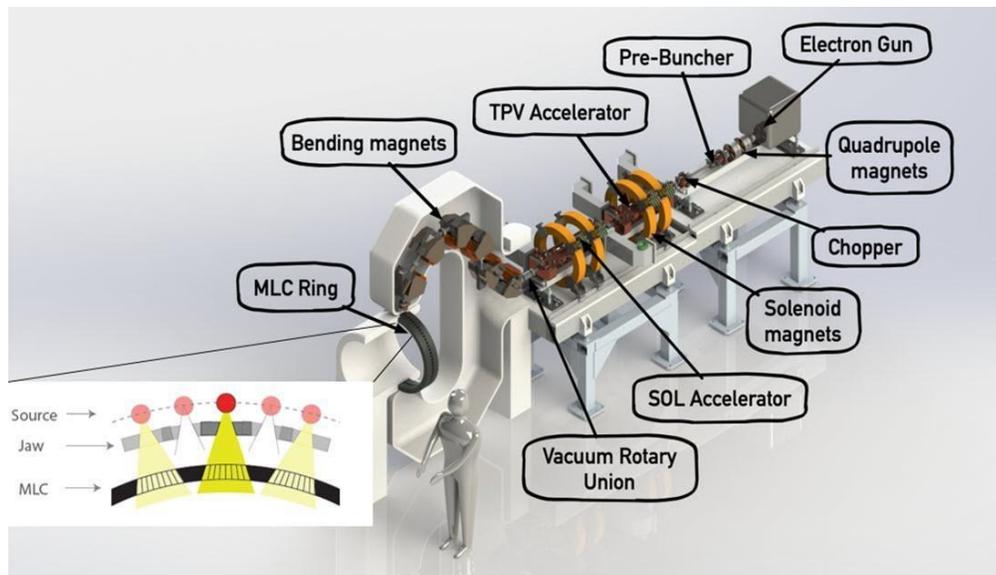
Figure 13. Rendering of the ROAD FLASH-RT system. A segment of the decoupled MLC ring is shown in the figure inset with three MLC modules. The linac is triggered to produce the beam when the target is aligned with the MLC to produce a VMAT-like treatment.
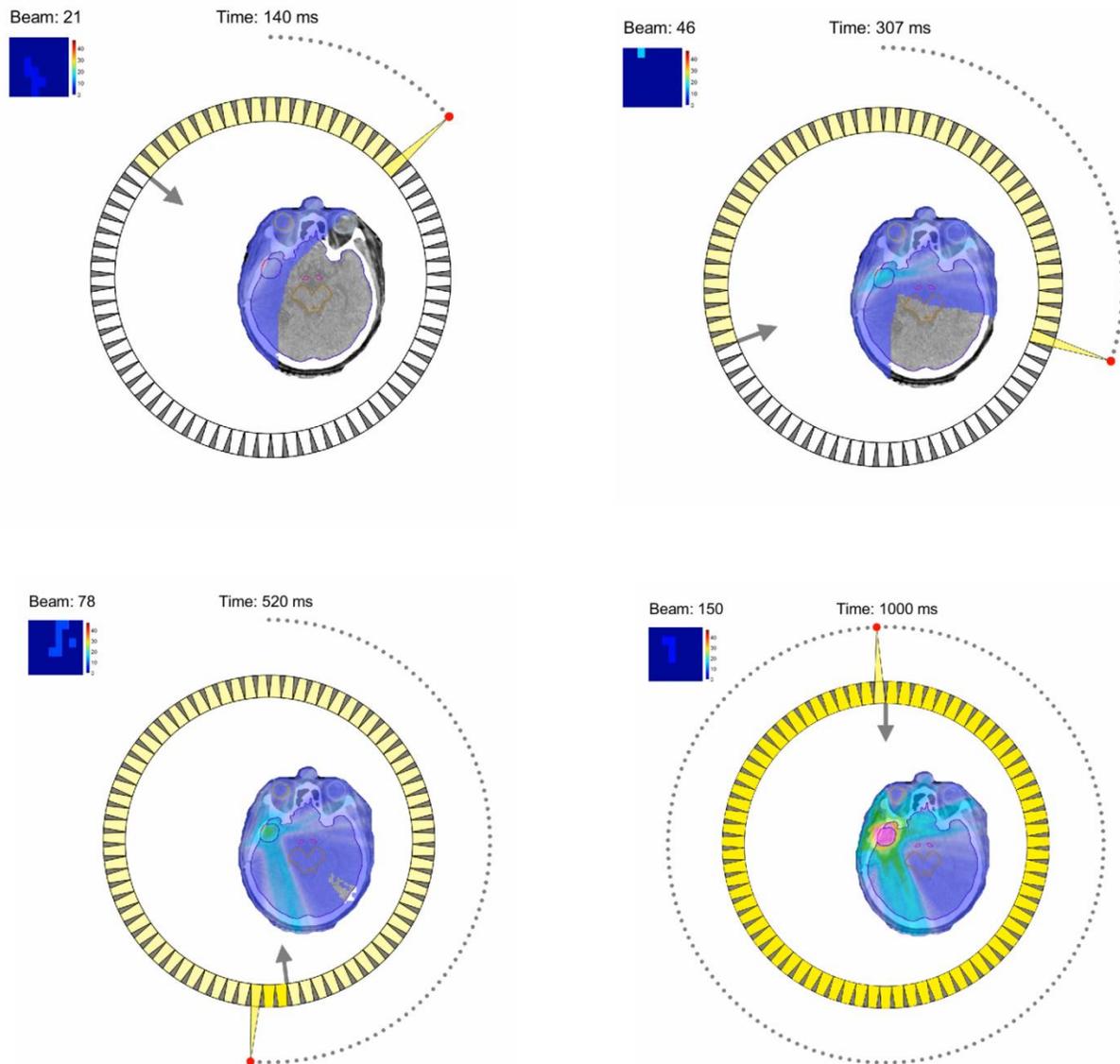
Figure 14. FLASH-RT delivery using ROAD. The figure shows four beams with the corresponding pre-shaped MLC in the upper left corner of respective beams. Cumulative radiation dose to a brain tumor patient is shown in the center.

Figure 14 shows the proposed delivery FLASH delivery using the ROAD method. There are a total of 75 MLC modules on a ring that is separate from the X-ray source. The X-ray pulses are triggered when the source is sequentially aligned with the MLC apertures. Counter-rotating the

MLC ring allows more aperture shapes to be programmed for further improved physical dose conformity.

With an increasing understanding of the underlying FLASH mechanism, it is necessary to further quantify the FLASH effect at the treatment planning stage as part of the inverse optimization goal. The feasibility has been demonstrated for simultaneous dose and dose rate optimization (SDDRO) with protons [117] and X-ray ROAD FLASH [116]. In the latter, the hypothesized oxygen depletion effect was parameterized into the planning system to show a larger FLASH effect for normal tissue sparing with larger individual pulses. The information will guide the design of high output and FLASH-ready linear accelerators.

3.6 Accelerator-based technology developed at SLAC National Accelerator Laboratory and Stanford University

3.6.1 X-ray FLASH-RT with the PHASER

The inherent inefficiency of producing therapeutic X-rays through bremsstrahlung radiation from an electron beam hitting a target contributes to the challenge of achieving FLASH dose rates with conventional photon radiotherapy. Another critical factor constraining the treatment time in a conventional radiotherapy device is the mechanical motion of the gantry. The PHASER program for Pluridirectional High-energy Agile Scanning Electronic Radiotherapy, led by SLAC National Accelerator Laboratory and Stanford Medical School, seeks to eliminate gantry motion while achieving the FLASH dose rate through a system of 16 linacs arrayed around the patient, as shown in Figure 15 [118]. This design enables multiple angles of approach, as needed for intensity modulated conformal radiation therapy. The PHASER program is intended to increase the

therapeutic index of radiotherapy through highly-conformal image guided FLASH treatments and improve the accessibility of state-of-the-art FLASH capable medical equipment through the implementation of a compact and economical design.
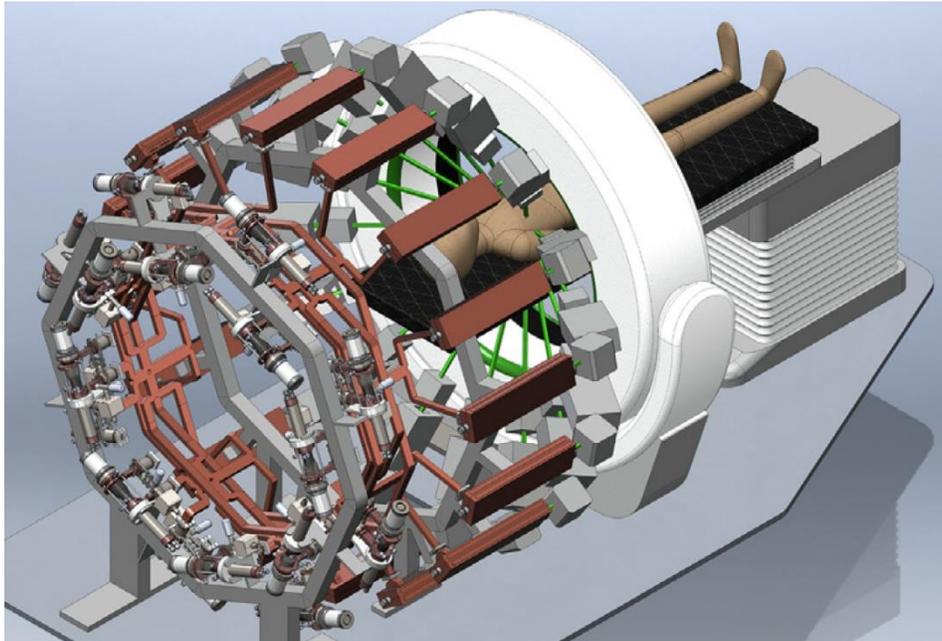
Figure 15. Conceptual diagram of the PHASER architecture with 16 linacs arrayed around the patient for highly conformal FLASH photon therapy.

PHASER seeks to achieve FLASH capability by producing a >400-fold increase in average beam current compared to conventional 10 MV photon therapy systems with a typical dose rate of 10 Gy/min. The linac structure will rely on a distributed coupling topology to improve the power efficiency, allowing the system to take advantage of a network of 16 compact "klystrinos," each producing a peak power of around 330 kW. The research and development from the initial PHASER program has laid the groundwork for extending the design concept to a Very High

Energy Electron (VHEE) therapy system, treating directly with ≥100 MeV electrons without x-ray conversion.

3.6.2   Very High Electron Energy (VHEE) FLASH-RT

Very High Energy Electron (VHEE) radiotherapy is a key area of opportunity to apply technology developed for the particle physics community to the new field of FLASH-RT. Direct use of an electron beam for radiotherapy provides one of the most readily scalable paths to achieve FLASH dose rates, as apparent in the existing body of experimental evidence for FLASH that has been predominantly performed with direct electron beams [1,5,119,120]. Existing facilities have been modified for FLASH radiotherapy experiments [121-123], and commercial systems like the Oriatron eRT6 from PMB-Alcen [124], Kinetron from CGRMeV [125], Novac7 from Sardina [126], and the Mobetron from IntraOp [127] have been employed for FLASH capability at sub-10 MeV electron energies. While clinical and pre-clinical commercial devices proceed with development to provide ultra-high-dose rate direct electron therapy [128,130], treatment of superficial tumors in human patients has already begun [2].

The key technological advance where active research is needed concerns the development of medical accelerators that can reach the high beam energies required to treat deep-seated tumors throughout the body. The electron beam energy determines the penetration depth, with a 100 MeV beam reaching a depth of about 40 cm, sufficient to cover almost all deep-seated tumors [131,132]. VHEE therapy has yet to be realized in a clinical setting because existing equipment lacks the capability to reach these beam energies. The maximum energy obtained for direct electron FLASH-RT thus far has been only 20 MeV, using a modified Varian Clinac [119,120]. The size

and power requirements to simply extend this structure to produce 100 MeV beams would be prohibitive for clinical use. The high beam energies used for VHEE treatments will also impose additional shielding requirements on the treatment facility. Treatment planning studies using Monte Carlo simulations indicate that a dose rate of approximately 2×10^4 Gy/s can be achieved per milliamp of average beam current over a 10 cm by 10 cm field size.

Current RF-driven linear accelerator research programs aimed at meeting the demand for VHEE capability have primarily focused on advanced, normal-conducting, high-gradient accelerator RF technology. A CHUV-CERN collaboration to build the DEFT (Deep Electron FLASH Therapy) facility plans to combine an X-band linac design developed through CLIC research with an S-band photoinjector [133]. Designs for a VHEE system at the PRAE accelerator utilize an S-band linac in addition to an S-band photoinjector, prioritizing linac performance reliability [134]. Implementation of a photoinjector with a medical linac has yet to be demonstrated, but the strategy of utilizing a photoinjector has already been proposed as an opportunity to harness the speed and flexibility of laser-based beam shaping techniques [118].

While the proposed DEFT facility will occupy a length of around ten meters, an R&D effort currently underway at SLAC National Accelerator Laboratory seeks to reach an even more compact VHEE system using a cryogenic X-band accelerator to achieve VHEE beam energies in only one meter. This approach harnesses the enhanced efficiency and higher gradient obtainable in a distributed coupling linac, combined with the improved scaling at cryogenic temperatures [135] to reach the target gradient of 100 MeV/ m, already demonstrated in previous experiments at SLAC using a cryogenic X-band structure at the X-band Test Area (XTA), see Figure 16 [136]. A key aspect of the proposed VHEE system is the reliance on a commercial RF source, limiting

the initial peak power to roughly 6 MW, but ensuring the final product can be widely adopted for commercial use. Advances in both the distributed coupling design and cryogenic operation of the normal conducting structure are necessary to maximize the power efficiency of the linac, allowing SLAC's one meter X-band structure to reach a gradient of 100 MeV/m while using a peak power of only 20 MW. A preliminary design of the cryogenic X-band linac is shown in Figure 17.
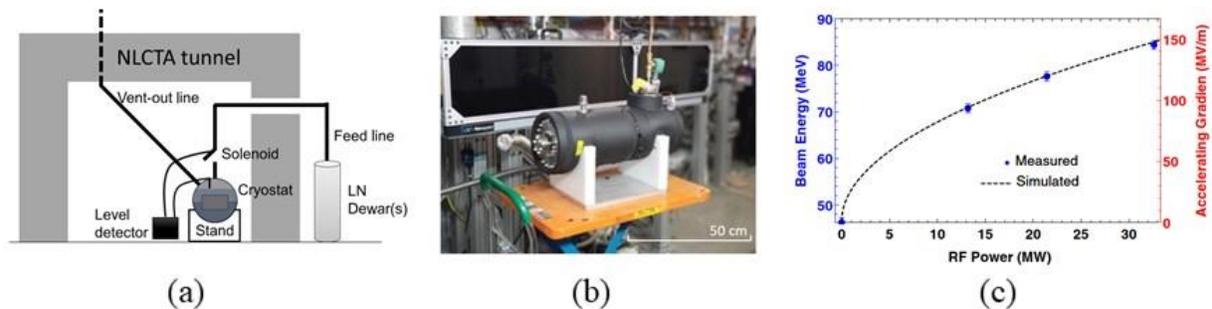
Figure 16. (a) Schematic of cryogenic test setup at XTA using liquid nitrogen. (b) Photo of linac and cryostat assembly prior to installation at XTA. (c) Measurements of accelerating gradient as a function of RF power from Ref. 137.

The SLAC system will rely on RF pulse compression to achieve a 20 MW peak power using the initial 6 MW pulse produced by the commercial klystron. RF pulse compression is a mature technology that has been used extensively for large scale accelerator applications to reconcile the need for short high-peak-power pulses with a cost-efficient long pulse, low power sources [137-139]. Recent advances in RF compressor technology have opened the door to compact structures that could dramatically reduce the system footprint while maintaining the capability to produce 4-fold pulse compression and isolate the source from the reflected RF signal from the cavities [140,141]. The SLAC VHEE program investigates multiple cavity designs, like the spherical cavity in Ref. 26, focusing on structures designed for high intrinsic quality factors, Q_0 up to 400,000, and high coupling factors, β up to 10. Active research in this area will continue to benefit efforts to design a new generation of compact, cost-efficient medical accelerators and the broader

accelerator community that relies on pulse compressors to supply the peak powers needed for high gradient operation.
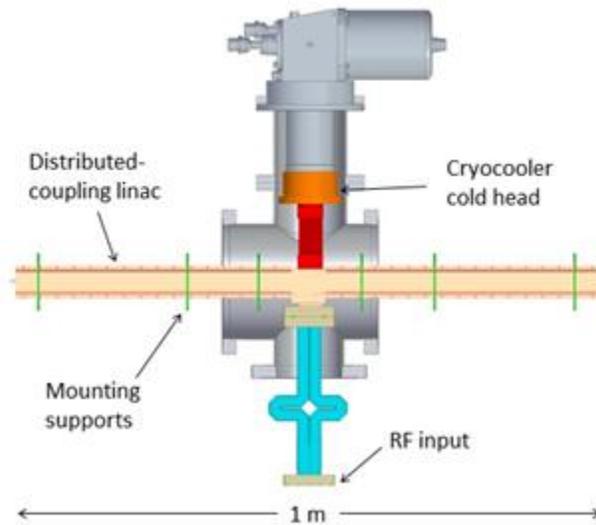
Figure 17. Schematic of the cryogenic X-band linac for VHEE under development at SLAC.

Proposed programs like the Cool Copper Collider (C^3) proposal [142] to realize an e^+e^- collider for the study of the Higgs boson offer an exciting opportunity for synergistic research efforts on accelerator technologies, from the distributed coupling linac to the pulse compression system, which could enhance power efficiency for a single compact cancer therapy system up to a large-scale facility like C^3. In each case, the same underlying techniques are used to push the limits on achievable accelerating gradients with a cost-efficient system. Research from a C^3 linac R&D effort [143] would provide insight into features needed for a high gradient VHEE system and vice versa, including stringent performance reliability criteria optimized for substantial beam current under cryogenic operating conditions.

Fabrication of SLAC's X-band distributed coupling linac for VHEE will rely on a split-block approach which allows significant flexibility for CNC machining of the linac cavities and power coupling manifold into the copper slabs. This flexibility is critical for implementing a 135° phase advance linac design which further enhances the power efficiency, increasing the shunt impedance by nearly 10% compared to the π-mode. On-going collaboration with industry partners will facilitate the transition of SLAC's prototype VHEE system into modular industrialized equipment. Mass-production will be an important feature not only for commercialization generally but also for achieving FLASH capability with the VHEE system. In order to eliminate gantry motion and reach an ultra-high dose rate, the proposed FLASH VHEE system utilizes an array of 16 linacs, in the same architecture as the PHASER system for photon therapy [118]

VHEE beam energies as high as 250 MeV could be needed for treatment scenarios that use advanced techniques like spatially fractionated radiotherapy in combination with FLASH dose rates [144]. The demand for equipment that can deliver these beam energies on the meter scale has motivated a search for technology that can provide gradients exceeding 100 MeV/m at the FLASH dose rate. Accelerators operating at even higher frequencies than X-band, up into the mm-wave regime, offer an opportunity to provide VHEE FLASH-RT with unprecedented compactness. Efforts are already underway at SLAC National Accelerator Laboratory to apply recent advances in mm-wave linac fabrication and high-power testing (Figure 18) to the design of a VHEE accelerator operating at 94 GHz [145].
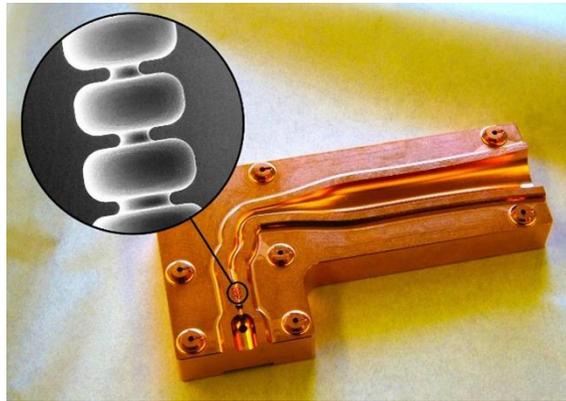
Figure 18. SLAC mm-wave linac prototype for high power testing.

The mm-wave and THz regime has long been frustratingly inaccessible for accelerator applications due to the absence of high-power sources and the challenges of implementing these small-scale structures. Motivated by the potential advantages of high frequency high gradient accelerators to explore the Energy Frontier, research has been conducted at SLAC on the fabrication of mm-wave accelerators [146] as well as methods of powering these structures and the physics of breakdown at these high frequencies [147]. New research is exploring the benefits of applying high gradient techniques like distributed coupling and cryogenic operation in the mm-wave regime [145,148]. These features offer the possibility for extremely power-efficient structures that could reach gradients of hundreds of MeV per meter. To power these structures, SLAC has partnered with the Air Force Research Laboratory to investigate active pulse compression at mm-wave frequencies, overcoming the limitations of low peak power available from commercial sources using techniques developed for nanosecond rf-power switching [149,150]. Active research and development is needed to push these structures beyond the few-cell prototypes that have undergone high power test to a full-scale system with demonstrated beam

acceleration. A critical area of research, particularly in the pursuit of FLASH dose rates, will be the design of an electron gun compatible with these mm-wave structures [151].

3.6.3 Fast 3D high-speed beam scanner for hadron FLASH-RT

Proton therapy, and hadron therapy in general, allows potentially far greater dose shaping control than conventional photon therapy or VHEE through the energy-dependent Bragg peak, which determines the depth at which the peak dose will be delivered. Proton cyclotron facilities for cancer therapy routinely alter the proton beam energy used in treatment by passing the beam through a so-called range shifter, a physical barrier of material, typically plastic, which reduces the beam energy according to the thickness of the plate. While the strategy is a reliable and robust method for changing the beam energy, the process of switching between range shifter settings is time-consuming, on the order of a second [152] when compared to the desired time scale of a total FLASH treatment that is a few hundred milliseconds, and also degrades the lateral penumbra of the beam. Synchrotron facilities, used for both proton and carbon cancer treatment, can change the beam energy by adjusting the acceleration cycling settings, avoiding the mechanical motion of a range shifter, but face challenges to achieving the FLASH dose rate. The demand for high-speed changes to beam energy presents a tantalizing opportunity to apply accelerator technology in which RF-driven energy modulation could accomplish the same objective as the range shifter with changes on the sub-µs scale.

This research thrust has already gained traction in a program at SLAC National Accelerator Laboratory to develop a 3D high-speed beam scanner for hadron therapy. The objectives of this project are to design and demonstrate the component technology needed to modulate the beam energy and transverse steering, sufficient to cover a 4-liter volume at a FLASH dose rate. The

energy modulator design builds on research concepts developed at SLAC for high energy physics applications, taking the high gradient capability of a distributed coupling S-band structure and using it to reach a +/- 30 MeV beam energy, equivalent to a range of 15 cm in treatment depth, in a one-meter structure [153].

SLAC's hadron scanning program tackles not only the challenge of RF-driven energy modulation but also transverse steering. Unlike conventional photon-based radiotherapy, VHEE and proton therapy allow for pencil beam scanning, which takes advantage of the Lorentz force to steer the charged particle trajectories. Thus far, transverse pencil beam scanning for protons has been routinely accomplished using electromagnets, which allow the beam to cover a large treatment field on the order of 30 cm by 40 cm at the patient isocenter [152,154]. This technique offers valuable flexibility in terms of coverage area with minimal beam distortion and, while not as fast as an RF-driven process, is compatible with the timescale of FLASH dose delivery. Changes to beam position can be accomplished on a few hundred microseconds scale [152]. Varian has already announced FLASH capability with their existing proton therapy equipment and has actively invested in FLASH therapy research through the FlashForward™ Consortium [155].
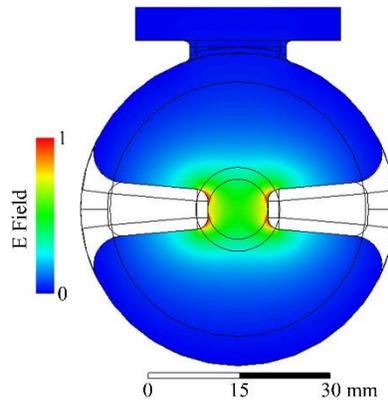
Figure 19. Electric field profile of the TE11-like mode shown in a cross-section of the deflector cell, with beam axis oriented into the page. The opposing posts (profiles shown in white) produce an RF dipole. Power is coupled in through the port at the top of the model simulated in ANSYS-HFSS.

These developments suggest that proton therapy will likely be one of the leading modalities for FLASH treatment in the near future. The ultrafast 3D beam shaping for hadron therapy championed by the SLAC-led collaboration on RF-driven beam manipulation offers an opportunity for the accelerator technology of the high energy physics community to revolutionize the speed and flexibility of proton therapy equipment. SLAC's proton deflector cavity, shown in Figure 19, is a prime example, taking inspiration from CERN's crab cavity research for beam steering [156] and optimizing a new cavity design for sub-relativistic protons [157]. The initial design for the SLAC 3D scanning system utilizes a few-cell deflector structure, with cavities oriented orthogonally for full range of transverse motion. The angular kick provided by the RF-driven deflector is enhanced by a set of static permanent magnet quadrupoles (PMQ). The effect of the PMQs will be to defocus in one plane and overfocus in the other. By compensating with the magnitude of the kick supplied by the deflector structure in each direction, this focusing action can be optimized for the maximum treatment area, covering around 15 cm x 22 cm for a proton beam energy of 200 MeV. This RF-driven approach to the proton beam modulation eliminates all

mechanical motion and allows for ultra-fast switching between different energies and lateral positions.

The initial SLAC research has focused on the design and demonstration of prototypes of both the energy modulator and deflector, with high power testing underway at SLAC's facilities. In order to realize this technology in clinical settings, research and development will be needed to build the full-scale accelerator structures and conduct testing with a proton beam. SLAC has partnered with Electron Energy Corporation (EEC) to investigate designs for the PMQ system used to enhance the treatment field covered by the SLAC RF deflector. EEC's research on cryogenic PMQ designs offers unique advantages in terms of flexibility and performance reliability over a range of cryogenic temperatures, with applications not only to potential proton therapy equipment but also to programs pushing the Energy Frontier like the C^3 proposal to develop an e^+e^- collider for the study of the Higgs boson [158].

4 Summary and Conclusions

FLASH radiation therapy (FLASH-RT) is the next frontier in radiation therapy for cancer. Initial preclinical and clinical research results look very promising, demonstrating enhanced protection of normal tissue, reduced toxicity and side effects, and good tumor control. Beam delivery questions remain, for example, the level of conformality or the use of multiple fields and intensity modulation, the role of the Bragg peak, possible limitations in tumor depth or size, and

the importance of low-dose regions. For non-pulsed or CW accelerators, does the RF bunch create a FLASH effect equivalent to the pulse structure of clinical electron accelerators?

The research thrust into FLASH has already gained momentum at the National Accelerator Laboratories and leading universities in the United States. There are several programs to develop new compact solutions for FLASH-dose rate capable machines delivering X-rays, electrons, protons, and ions, with a comprehensive overview presented in this white paper. In addition to high-intensity accelerator R&D, precision beam control will need to be enhanced by a factor of 20-50 over a large field with corresponding and unprecedented ultra-fast detector response time and linearity. Investment into research and development and close collaboration between national accelerator labs, industry, and academic medical institutions will be required to realize and transfer the new technologies in clinical settings.

References

[1]   Favaudon V, Caplier L, Monceau V, Pouzoulet F, Sayarath M, Fouillade C, Poupon MF, Brito I, Hupé P, Bourhis J, Hall J, Fontaine JJ, Vozenin MC. Ultrahigh dose-rate FLASH irradiation increases the differential response between normal and tumor tissue in mice. Sci Transl Med. 2014 Jul 16;6(245):245ra93. doi: 10.1126/scitranslmed.3008973. Erratum in: Sci Transl Med. 2019 Dec 18;11(523): PMID: 25031268.

[2]   Bourhis J, Sozzi WJ, Jorge PG, Gaide O, Bailat C, Duclos F, Patin D, Ozsahin M, Bochud F, Germond JF, Moeckli R, Vozenin MC. Treatment of a first patient with FLASH-radiotherapy. Radiother Oncol. 2019 Oct;139:18-22. doi: 10.1016/j.radonc.2019.06.019. Epub 2019 Jul 11. PMID: 31303340.

[3]   Wei S, Lin H, Choi JI, Simone CB 2nd, Kang M. A Novel Proton Pencil Beam Scanning FLASH-RT Delivery Method Enables Optimal OAR Sparing and Ultra-High Dose Rate Delivery: A Comprehensive Dosimetry Study for Lung Tumors. Cancers (Basel). 2021 Nov 18;13(22):5790. doi: 10.3390/cancers13225790. PMID: 34830946; PMCID: PMC8616118.

[4]   Wei S, Lin H, Choi JI, Press RH, Lazarev S, Kabarriti R, Hajj C, Hasan S, Chhabra AM, Simone CB 2nd, Kang M. FLASH Radiotherapy Using Single-Energy Proton PBS Transmission Beams for Hypofractionation Liver Cancer: Dose and Dose Rate

Quantification. Front Oncol. 2022 Jan 13;11:813063. doi: 10.3389/fonc.2021.813063. PMID: 35096620; PMCID: PMC8794777.

[5]   Montay-Gruel P, Petersson K, Jaccard M, Boivin G, Germond JF, Petit B, Doenlen R, Favaudon V, Bochud F, Bailat C, Bourhis J, Vozenin MC. Irradiation in a flash: Unique sparing of memory in mice after whole brain irradiation with dose rates above 100Gy/s. Radiother Oncol. 2017 Sep;124(3):365-369. doi: 10.1016/j.radonc.2017.05.003. Epub 2017 May 22. PMID: 28545957.

[6]   Harrington KJ. Ultrahigh Dose-rate Radiotherapy: Next Steps for FLASH-RT. Clin Cancer Res. 2019 Jan 1;25(1):3-5. doi: 10.1158/1078-0432.CCR-18-1796. Epub 2018 Aug 9. PMID: 30093447.

[7]   Wilson JD, Hammond EM, Higgins GS, Petersson K. Ultra-High Dose Rate (FLASH) Radiotherapy: Silver Bullet or Fool's Gold? Front Oncol. 2020 Jan 17;9:1563. doi: 10.3389/fonc.2019.01563. Erratum in: Front Oncol. 2020 Feb 25;10:210. PMID: 32010633; PMCID: PMC6979639.

[8]   Montay-Gruel P, Acharya MM, Gonçalves Jorge P, Petit B, Petridis IG, Fuchs P, Leavitt R, Petersson K, Gondré M, Ollivier J, Moeckli R, Bochud F, Bailat C, Bourhis J, Germond JF, Limoli CL, Vozenin MC. Hypofractionated FLASH-RT as an Effective Treatment against Glioblastoma that Reduces Neurocognitive Side Effects in Mice. Clin Cancer Res. 2021 Feb 1;27(3):775-784. doi: 10.1158/1078-0432.CCR-20-0894. Epub 2020 Oct 15. PMID: 33060122; PMCID: PMC7854480.

[9]   Berry RJ, Hall EJ, Forster DW, Storr TH, Goodman MJ. Survival of mammalian cells exposed to x rays at ultra-high dose-rates. Br J Radiol. 1969 Feb;42(494):102-7. doi: 10.1259/0007-1285-42-494-102. PMID: 4975207.

[10]   Bazalova-Carter M, Esplen N. On the capabilities of conventional x-ray tubes to deliver ultra-high (FLASH) dose rates. Med Phys. 2019 Dec;46(12):5690-5695. doi: 10.1002/mp.13858. Epub 2019 Oct 23. PMID: 31600830.

[11]   Gao F, Yang Y, Zhu H, Wang J, Xiao D, Zhou Z, Dai T, Zhang Y, Feng G, Li J, Lin B, Xie G, Ke Q, Zhou K, Li P, Shen X, Wang H, Yan L, Lao C, Shan L, Li M, Lu Y, Chen M, Feng S, Zhao J, Wu D, Du X. First demonstration of the FLASH effect with ultrahigh dose rate high-energy X-rays. Radiother Oncol. 2022 Jan;166:44-50. doi: 10.1016/j.radonc.2021.11.004. Epub 2021 Nov 11. PMID: 34774651.

[12]   Smyth LML, Donoghue JF, Ventura JA, Livingstone J, Bailey T, Day LRJ, Crosbie JC, Rogers PAW. Comparative toxicity of synchrotron and conventional radiation therapy based on total and partial body irradiation in a murine model. Sci Rep. 2018 Aug 13;8(1):12044. doi: 10.1038/s41598-018-30543-1. PMID: 30104646; PMCID: PMC6089899.

[13]   Montay-Gruel P, Bouchet A, Jaccard M, Patin D, Serduc R, Aim W, Petersson K, Petit B, Bailat C, Bourhis J, Bräuer-Krisch E, Vozenin MC. X-rays can trigger the FLASH effect: Ultra-high dose-rate synchrotron light source prevents normal brain

injury after whole brain irradiation in mice. Radiother Oncol. 2018 Dec;129(3):582-588. doi: 10.1016/j.radonc.2018.08.016. Epub 2018 Aug 31. PMID: 30177374.

[14]   Cunningham S, McCauley S, Vairamani K, Speth J, Girdhani S, Abel E, Sharma RA, Perentesis JP, Wells SI, Mascia A, Sertorio M. FLASH Proton Pencil Beam Scanning Irradiation Minimizes Radiation-Induced Leg Contracture and Skin Toxicity in Mice. Cancers (Basel). 2021 Mar 1;13(5):1012. doi: 10.3390/cancers13051012. PMID: 33804336; PMCID: PMC7957631.

[15]   Beyreuther E, Brand M, Hans S, Hideghéty K, Karsch L, Leßmann E, Schürer M, Szabó ER, Pawelke J. Feasibility of proton FLASH effect tested by zebrafish embryo irradiation. Radiother Oncol. 2019 Oct;139:46-50. doi: 10.1016/j.radonc.2019.06.024. Epub 2019 Jun 29. PMID: 31266652.

[16]   R. W. Hamm et al, "Preliminary Design of a Dedicated Proton Therapy Linac", Proceedings of PAC-1991 Conference, San Francisco, CA, May 1991.

[17]   U. Amaldi et al, "Proton and Carbon Linacs for Hadron Therapy", Proceedings of LINAC-2014 Conference, Geneva, Switzerland, September 2014.

[18]   P. Ostroumov et al, "Compact Carbon Ion Linac", Proceedings of NAPAC-2016 Conference, Chicago, IL, October 10-14, 2016.

[19]   Ungaro D, Degiovanni A, Stabile P, "LIGHT: A Linear Accelerator for Proton Therapy". In: Proceedings of north american particle accelerator conference (NAPAC'16), Chicago, IL, USA, October 9–14, 2017. p. 1282–86. doi:10.18429/JACoWNAPAC2016-FRB1IO02.

[20]   S. Jolly et al, Physica Medica 78 (2020) 71–82

[21]   S. Benedetti et al, "RF Design of A Novel S-Band Backward Travelling Wave Linac for Proton Therapy", Proceedings of LINAC-2014, Geneva, Switzerland.

[22]   S. Kutsaev et al, "High-Gradient Low-β Accelerating Structure Using the First Negative Harmonic of the Fundamental Mode", Physical Review Accelerators and Beams 20 (2017) 120401

[23]   S. Kutsaev et al, "Test Results of a High-Gradient 2.856 GHz Negative Harmonic Accelerating Waveguide", IEEE Microwave and Wireless Components Letters, DOI 10.1109/LMWC.2021.3081358.

[24]   B. Mustapha et al, "Design of a High-Gradient S-Band Annular Coupled Structure", NAPAC-2019 Conference Proceedings, September 1-6, 2019, Lansing, MI.

[25]   B. Mustapha et al, "Prospects for an Advanced Heavy Ion Therapy Center in the Chicago Area", AIP Conference Proceedings 2160, 050009 (2019); https://doi.org/10.1063/1.5127701

[26]   J. Van de Walle, et al.: THE S2C2: FROM SOURCE TO EXTRACTION. Proceedings of Cyclotrons2016, Zurich, Switzerland,THB01. https://accelconf.web.cern.ch/cyclotrons2016/papers/thb01.pdf

[27]   M. Yoshimoto, et al.: Recent beam studies of the POP FFAG proton synchrotron. Proceedings of the 2001 Particle Accelerator Conference, Chicago. https://accelconf.web.cern.ch/p01/PAPERS/MOPA012.PDF

[28]   Y. Yonemura, et al.: Development of ffag accelerator at KEK. Proceedings of 2005 Particle Accelerator Conference, Knoxville, Tennessee. https://accelconf.web.cern.ch/p05/PAPERS/FPAE026.PDF

[29]   Antoine, S et al. "Principle Design of a Protontherapy, Rapid-Cycling, Variable Energy Spiral FFAG." Nuclear instruments & methods in physics research. Section A, Accelerators, spectrometers, detectors and associated equipment 602.2 (2009): 293–305.

[30]   Planche, T et al. "Design of a Prototype Gap Shaping Spiral Dipole for a Variable Energy Protontherapy FFAG." Nuclear instruments & methods in physics research. Section A, Accelerators, spectrometers, detectors and associated equipment 604.3 (2009): 435–442.

[31]   F. Méot: RACCAM, A status, including magnet prototyping, magnetic measurements. FFAG 2009 workshop, Fermilab, Batavia, IL, USA. https://indico.fnal.gov/event/2672/contributions/77834/attachments/48652/58457/FM eot1-090921.pdf

[32]   Johnstone, C. et al. "High-Current Light-Ion Cyclotron for Applications in Nuclear Security and Radioisotope Production." IEEE transactions on nuclear science 68.5 (2021): 1072–1082.

[33]   Kutsaev, Sergey V et al. "Electromagnetic and Engineering Design of a High-Current 15-MeV/u Cyclotron." IEEE transactions on nuclear science 68.5 (2021): 1083–1093.

[34]   Bulanov S V., Esirkepov T, Khoroshkov VS, Kuznetsov A V., Pegoraro F. Oncological hadrontherapy with laser ion accelerators. Phys Lett Sect A Gen At Solid State Phys. 2002;299(2–3):240–7.

[35]   C. Emma et al. Snowmass2021 Accelerator Frontier White Paper: Near Term Applications driven by Advanced Accelerator Concepts. Proceedings of the US Community Study on the Future of Particle Physics (Snowmass 2021)

[36]   Strickland D, Mourou G. Compression of amplified chirped optical pulses. Opt Commun. 1985;55(6):447–9.

[37]   Nakamura K, Mao HS, Gonsalves AJ, Vincenti H, Mittelberger DE, Daniels J, Magana A, Toth C, Leemans WP. Diagnostics, Control and Performance Parameters for the BELLA High Repetition Rate Petawatt Class Laser. IEEE J Quantum Electron. 2017;53(4):1200121.

[38]   Tajima T, Dawson JM. Laser Electron Accelerator. Phys Rev Lett. 1979 Jul;43(4):267–70.

[39]   Wilks SC, Langdon AB, Cowan TE, Roth M, Singh M, Hatchett S, Key MH, Pennington D, Mackinnon A, Snavely RA. Energetic proton generation in ultra-intense laser--solid interactions. Phys Plasmas. 2001;8(2):542–9.

[40]   Wang X, Zgadzaj R, Fazel N, Li Z, Yi SA, Zhang X, Henderson W, Chang Y-Y, Korzekwa R, Tsai H-E, Pai C-H, Quevedo H, Dyer G, Gaul E, Martinez M, Bernstein AC, Borger T, Spinks M, Donovan M, Khudik V, Shvets G, Ditmire T, Downer MC. Quasi-monoenergetic laser-plasma acceleration of electrons to 2 GeV. Nat Commun. 2013 Dec 11;4(1):1988.

[41]   Leemans WP, Gonsalves AJ, Mao H-S, Nakamura K, Benedetti C, Schroeder CB, Tóth C, Daniels J, Mittelberger DE, Bulanov SS, Vay J-L, Geddes CGR, Esarey E. Multi-GeV Electron Beams from Capillary-Discharge-Guided Subpetawatt Laser Pulses in the Self-Trapping Regime. Phys Rev Lett. 2014;113(24):245002.

[42]   Couperus JP, Pausch R, Köhler A, Zarini O, Krämer JM, Garten M, Huebl A, Gebhardt R, Helbig U, Bock S, Zeil K, Debus A, Bussmann M, Schramm U, Irman A. Demonstration of a beam loaded nanocoulomb-class laser wakefield accelerator. Nat Commun. 2017;8(1):487.

[43]   Gonsalves AJ, Nakamura K, Daniels J, Benedetti C, Pieronek C, de Raadt TCH, Steinke S, Bin JH, Bulanov SS, van Tilborg J, Geddes CGR, Schroeder CB, Tóth C, Esarey E, Swanson K, Fan-Chiang L, Bagdasarov G, Bobrova N, Gasilov V, Korn G, Sasorov P, Leemans WP. Petawatt Laser Guiding and Electron Beam Acceleration to 8 GeV in a Laser-Heated Capillary Discharge Waveguide. Phys Rev Lett. 2019;122(8):084801.

[44]   Leemans WP, Geddes CGR, Faure J, Tóth C, van Tilborg J, Schroeder CB, Esarey E, Fubiani G, Auerbach D, Marcelis B, Carnahan MA, Kaindl RA, Byrd J, Martin MC. Observation of Terahertz Emission from a Laser-Plasma Accelerated Electron Bunch Crossing a Plasma-Vacuum Boundary. Phys Rev Lett. 2003 Aug 14;91(7):074802.

[45]   Powers ND, Ghebregziabher I, Golovin G, Liu C, Chen S, Banerjee S, Zhang J, Umstadter DP. Quasi-monoenergetic and tunable X-rays from a laser-driven Compton light source. Nat Photonics. 2014 Jan 24;8(1):28–31.

[46]   Ta Phuoc K, Corde S, Thaury C, Malka V, Tafzi A, Goddet JP, Shah RC, Sebban S, Rousse A. All-optical Compton gamma-ray source. Nat Photonics. 2012 May 22;6(5):308–11.

[47]   Snavely RA, Key MH, Hatchett SP, Cowan TE, Roth M, Phillips TW, Stoyer MA, Henry EA, Sangster TC, Singh MS, Wilks SC, MacKinnon A, Offenberger A, Pennington DM, Yasuike K, Langdon AB, Lasinski BF, Johnson J, Perry MD, Campbell EM. Intense High-Energy Proton Beams from Petawatt-Laser Irradiation of Solids. Phys Rev Lett. 2000;85(14):2945–8.

[48]   Hatchett SP, Brown CG, Cowan TE, Henry EA, Johnson JS, Key MH, Koch JA, Langdon AB, Lasinski BF, Lee RW, Mackinnon AJ, Pennington DM, Perry MD, Phillips TW, Roth M, Sangster TC, Singh MS, Snavely RA, Stoyer MA, Wilks SC,

Yasuike K. Electron, photon, and ion beams from the relativistic interaction of Petawatt laser pulses with solid targets. Phys Plasmas. 2000;7(5):2076–82.

[49]   Steinke S, Bin JH, Park J, Ji Q, Nakamura K, Gonsalves AJ, Bulanov SS, Thévenet M, Toth C, Vay J-L, Schroeder CB, Geddes CGR, Esarey E, Schenkel T, Leemans WP. Acceleration of high charge ion beams with achromatic divergence by petawatt laser pulses. Phys Rev Accel Beams. 2020 Feb 19;23(2):021302.

[50]   Higginson A, Gray RJ, King M, Dance RJ, Williamson SDR, Butler NMH, Wilson R, Capdessus R, Armstrong C, Green JS, Hawkes SJ, Martin P, Wei WQ, Mirfayzi SR, Yuan XH, Kar S, Borghesi M, Clarke RJ, Neely D, McKenna P. Near-

[51]   Schreiber J, Bolton PR, Parodi K. Invited Review Article: "Hands-on" laser-driven ion acceleration: A primer for laser-driven source development and potential applications. Rev Sci Instrum. 2016;87(7):71101.100 MeV protons via a laser-driven transparency-enhanced hybrid acceleration scheme. Nat Commun. 2018 Dec 20;9(1):724.

[52]   Macchi A, Borghesi M, Passoni M. Ion acceleration by superintense laser-plasma interaction. Rev Mod Phys. 2013;85(2):751–93.

[53]   Daido H, Nishiuchi M, Pirozhkov AS. Review of laser-driven ion sources and their applications. Reports Prog Phys. 2012;75(5):56401.

[54]   Friedl AA, Prise KM, Butterworth KT, Montay-Gruel P, Favaudon V. Radiobiology of the FLASH effect. Med Phys. 2021;(May):1–21.

[55]   Friedl AA, Schmid TE. Application of Laser- Driven Beams for Radiobiological Experiments. In: Bolton PR, Parodi K, Schreiber J, editors. Applications of Laser-Driven Particle Acceleration. CRC Press; 2018. p. 129–38.

[56]   Durante M. New challenges in high-energy particle radiobiology. Br J Radiol. 2014 Mar 1;87(1035).

[57]   Yogo A, Sato K, Nishikino M, Mori M, Teshima T, Numasaki H, Murakami M, Demizu Y, Akagi S, Nagayama S, Ogura K, Sagisaka A, Orimo S, Nishiuchi M, Pirozhkov AS, Ikegami M, Tampo M, Sakaki H, Suzuki M, Daito I, Oishi Y, Sugiyama H, Kiriyama H, Okada H, Kanazawa S, Kondo S, Shimomura T, Nakai Y, Tanoue M, Sasao H, Wakai D, Bolton PR, Daido H. Application of laser-accelerated protons to the demonstration of DNA double-strand breaks in human cancer cells. Appl Phys Lett. 2009 May 7;94(18):181502.

[58]   Kraft SD, Richter C, Zeil K, Baumann M, Beyreuther E, Bock S, Bussmann M, Cowan TE, Dammene Y, Enghardt W, Heibig U, Karsch L, Kluge T, Laschinsky L, Lessmann E, Metzkes J, Naumburger D, Sauerbrey R, Schürer M, Sobiella M, Woithe J, Schramm U, Pawelke J. Dose-dependent biological damage of tumour cells by laser-accelerated proton beams. New J Phys. 2010;12:085003.

[59]   Yogo A, Maeda T, Hori T, Sakaki H, Ogura K, Nishiuchi M, Sagisaka A, Kiriyama H, Okada H, Kanazawa S, Shimomura T, Nakai Y, Tanoue M, Sasao F, Bolton PR,

Murakami M, Nomura T, Kawanishi S, Kondo K. Measurement of relative biological effectiveness of protons in human cancer cells using a laser-driven quasimonoenergetic proton beamline. Appl Phys Lett. 2011;98(5):2009–12.

[60]   Bin J, Allinger K, Assmann W, Dollinger G, Drexler GA, Friedl AA, Habs D, Hilz P, Hoerlein R, Humble N, Karsch S, Khrennikov K, Kiefer D, Krausz F, Ma W, Michalski D, Molls M, Raith S, Reinhardt S, Röper B, Schmid TE, Tajima T, Wenz J, Zlobinskaya O, Schreiber J, Wilkens JJ. A laser-driven nanosecond proton source for radiobiological studies. Appl Phys Lett. 2012;101(24).

[61]   Doria D, Kakolee KF, Kar S, Litt SK, Fiorini F, Ahmed H, Green S, Jeynes JCG, Kavanagh J, Kirby D, Kirkby KJ, Lewis CL, Merchant MJ, Nersisyan G, Prasad R, Prise KM, Schettino G, Zepf M, Borghesi M. Biological effectiveness on live cells of laser driven protons at dose rates exceeding 109 Gy/s. AIP Adv. 2012 Mar 1;2(1).

[62]   Raschke S, Spickermann S, Toncian T, Swantusch M, Boeker J, Giesen U, Iliakis G, Willi O, Boege F. Ultra-short laser-accelerated proton pulses have similar DNA-damaging effectiveness but produce less immediate nitroxidative stress than conventional proton beams. Sci Rep. 2016 Aug 31;6(1):1–9.

[63]   Manti L, Perozziello FM, Borghesi M, Candiano G, Chaudhary P, Cirrone GAP, Doria D, Gwynne D, Leanza R, Prise KM, Romagnani L, Romano F, Scuderi V, Tramontana A. The radiobiology of laser-driven particle beams: Focus on sub-lethal responses of normal human cells. In: Journal of Instrumentation. Manti2017: Institute of Physics Publishing; 2017. p. C03084.

[64]   Bayart E, Flacco A, Delmas O, Pommarel L, Levy D, Cavallone M, Megnin-Chanet F, Deutsch E, Malka V. Fast dose fractionation using ultra-short laser accelerated proton pulses can increase cancer cell mortality, which relies on functional PARP1 protein. Sci Rep. 2019;9(1):1–10.

[65]   Hanton F, Chaudhary P, Doria D, Gwynne D, Maiorino C, Scullion C, Ahmed H, Marshall T, Naughton K, Romagnani L, Kar S, Schettino G, McKenna P, Botchway S, Symes DR, Rajeev PP, Prise KM, Borghesi M. DNA DSB Repair Dynamics following Irradiation with Laser-Driven Protons at Ultra-High Dose Rates. Sci Rep. 2019 Dec 1;9(1):1–10.

[66]   Rösch TF, Szabó Z, Haffa D, Bin J, Brunner S, Englbrecht FS, Friedl AA, Gao Y, Hartmann J, Hilz P, Kreuzer C, Lindner FH, Ostermayr TM, Polanek R, Speicher M, Szabó ER, Taray D, Tokés T, Würl M, Parodi K, Hideghéty K, Schreiber J. A feasibility study of zebrafish embryo irradiation with laser-accelerated protons. Rev Sci Instrum. 2020 Jun 9;91(6):063303.

[67]   Han J, Mei Z, Lu C, Qian J, Liang Y, Sun X, Pan Z, Kong D, Xu S, Liu Z, Gao Y, Qi G, Shou Y, Chen S, Cao Z, Zhao Y, Lin C, Zhao Y, Geng Y, Chen J, Yan X, Ma W, Yang G. Ultra-High Dose Rate FLASH Irradiation Induced Radio-Resistance of Normal Fibroblast Cells Can Be Enhanced by Hypoxia and Mitochondrial

Dysfunction Resulting From Loss of Cytochrome C. Front Cell Dev Biol. 2021;9:1–11.

[68]   Bin J, Obst-Huebl L, Mao J-H, Nakamura K, Geulig LD, Chang H, Ji Q, He L, De Chant J, Kober Z, Gonsalves AJ, Bulanov S, Celniker SE, Schroeder CB, Geddes CGR, Esarey E, Simmons BA, Schenkel T, Blakely EA, Steinke S, Snijders AM. A new platform for ultra-high dose rate radiobiological research using the BELLA PW laser proton beamline. Sci Rep. 2022 Jan 27;12:1484.

[69]   Laschinsky L, Baumann M, Beyreuther E, Enghardt W, Kaluza M, Karsch L, Lessmann E, Naumburger D, Nicolai M, Richter C, Sauerbrey R, Schlenvoigt HP, Pawelke J. Radiobiological effectiveness of laser accelerated electrons in comparison to electron beams from a conventional linear accelerator. J Radiat Res. 2012;53(3):395–403.

[70]   Labate L, Andreassi MG, Baffigi F, Basta G, Bizzarri R, Borghini A, Candiano GC, Casarino C, Cresci M, Di Martino F, Fulgentini L, Ghetti F, Gilardi MC, Giulietti A, Köster P, Lenci F, Levato T, Oishi Y, Russo G, Sgarbossa A, Traino C, Gizzi LA. Small-scale laser based electron accelerators for biology and medicine: a comparative study of the biological effectiveness. Laser Accel Electrons, Protons, Ions II; Med Appl Laser-Generated Beams Part II; Harnessing Relativ Plasma Waves III. 2013;8779:87790O.

[71]   Oppelt M, Baumann M, Bergmann R, Beyreuther E, Brüchner K, Hartmann J, Karsch L, Krause M, Laschinsky L, Leßmann E, Nicolai M, Reuter M, Richter C, Sävert A, Schnell M, Schürer M, Woithe J, Kaluza M, Pawelke J. Comparison study of in vivo dose response to laser-driven versus conventional electron beam. Radiat Environ Biophys 2015 542. 2015 Jan 20;54(2):155–66.

[72]   Andreassi MG, Borghini A, Pulignani S, Baffigi F, Fulgentini L, Koester P, Cresci M, Vecoli C, Lamia D, Russo G, Panetta D, Tripodi M, Gizzi LA, Labate L. Radiobiological Effectiveness of Ultrashort Laser-Driven Electron Bunches: Micronucleus Frequency, Telomere Shortening and Cell Viability. Radiat Res. 2016 Sep 1;186(3):245–53.

[73]   Babayan N, Grigoryan B, Khondkaryan L, Tadevosyan G, Sarkisyan N, Grigoryan R, Apresyan L, Aroutiounian R, Vorobyeva N, Pustovalova M, Grekhova A, Osipov AN. Laser-Driven Ultrashort Pulsed Electron Beam Radiation at Doses of 0.5 and 1.0 Gy Induces Apoptosis in Human Fibroblasts. Int J Mol Sci 2019, Vol 20, Page 5140. 2019 Oct 17;20(20):5140.

[74]   Cavallone M, Rovige L, Huijts J, Bayart É, Delorme R, Vernier A, Jorge PG, Moeckli R, Deutsch E, Faure J, Flacco A. Dosimetric characterisation and application to radiation biology of a kHz laser-driven electron beam. Appl Phys B Lasers Opt. 2021;127(4):1–8.

[75]   DesRosiers C, Moskvin V, Bielajew AF, Papiez L. 150-250 MeV electron beams in radiation therapy. Phys Med Biol. 2000;45(7):1781–805.

[76]   Kokurewicz K, Welsh GH, Brunetti E, Wiggins SM, Boyd M, Sorensen A. Laser-plasma generated very high energy electrons (VHEEs) in radiotherapy. In: Proc of SPIE. 2017. p. 102390C-1–9.

[77]   Labate L, Palla D, Panetta D, Avella F, Baffigi F, Brandi F, Di Martino F, Fulgentini L, Giulietti A, Köster P, Terzani D, Tomassini P, Traino C, Gizzi LA. Toward an effective use of laser-driven very high energy electrons for radiotherapy: Feasibility assessment of multi-field and intensity modulation irradiation schemes. Sci Rep. 2020 Dec 14;10(1):17307.

[78]   Svendsen K, Guénot D, Svensson JB, Petersson K, Persson A, Lundh O. A focused very high energy electron beam for fractionated stereotactic radiotherapy. Sci Rep. 2021;11(1):1–8.

[79]   Pommarel L, Vauzour B, Bayart E, Delmas O, Goudjil F, Nauraye C, Letellier V, Pouzoulet F, Schillaci F, Romano F, Scuderi V, Cirrone GAP, Deutsch E, Flacco A, Malka V. Spectral and spatial shaping of a laser-produced ion beam for radiation-biology experiments. 2017;032801:1–10.

[80]   Brack FE, Kroll F, Gaus L, Bernert C, Beyreuther E, Cowan TE, Karsch L, Kraft S, Kunz-Schughart LA, Lessmann E, Metzkes-Ng J, Obst-Huebl L, Pawelke J, Rehwald M, Schlenvoigt HP, Schramm U, Sobiella M, Szabó ER, Ziegler T, Zeil K. Spectral and spatial shaping of laser-driven proton beams using a pulsed high-field magnet beamline. Sci Rep. 2020 Dec 1;10:9118.

[81]   Cirrone GAP, Petringa G, Catalano R, Schillaci F, Allegra L, Amato A, Avolio R, Costa M, Cuttone G, Fajstavr A, Gallo G, Giuffrida L, Guarrera M, Korn G, Larosa G, Leanza R, Lo Vecchio E, Messina G, Milluzzo G, Olsovcova V, Pulvirenti S, Pipek J, Romano F, Rizzo D, Russo AD, Salamone S, Scuderi V, Velyhan A, Vinciguerra S, Zakova M, Zappalà E, Margarone D. ELIMED-ELIMAIA: The First Open User Irradiation Beamline for Laser-Plasma-Accelerated Ion Beams. Front Phys. 2020 Nov 13;8:564907.

[82]   Brüchner K, Beyreuther E, Baumann M, Krause M, Oppelt M, Pawelke J. Establishment of a small animal tumour model for in vivo studies with low energy laser accelerated particles. Radiat Oncol. 2014;9(1):1–9.

[83]   Tilborg J Van, Steinke S, Geddes CGR, Matlis NH, Shaw BH, Gonsalves AJ, Huijts J V, Nakamura K, Daniels J, Schroeder CB, Benedetti C, Esarey E, Bulanov SS, Bobrova NA, Sasorov P V, Leemans WP. Active Plasma Lensing for Relativistic Laser-Plasma-Accelerated Electron Beams. Phys Rev Lett. 2015;115(October):184802.

[84]   Linz U, Alonso J. Laser-driven ion accelerators for tumor therapy revisited. Phys Rev Accel Beams. 2016;19(12):124802.

[85]   Enghardt W, Pawelke J, Wilkens JJ. Laser-Driven Ion Beam Radiotherapy (LIBRT). In: Bolton PR, Parodi K, Schreiber J, editors. Applications of Laser-Driven Particle Acceleration. CRC Press; 2018. p. 165–82.

[86]   Masood U, Cowan TE, Enghardt W, Hofmann KM, Karsch L, Kroll F, Schramm U, Wilkens JJ, Pawelke J. A light-weight compact proton gantry design with a novel dose delivery system for broad-energetic laser-accelerated beams. Phys Med Biol. 2017 Jun 13;62(13):5531–55.

[87]   Hofmann KM, Masood U, Pawelke J, Wilkens JJ. A treatment planning study to assess the feasibility of laser-driven proton therapy using a compact gantry design. Med Phys. 2015;42(9):5120–9.

[88]   Gotz M, Karsch L, Pawelke J. A new model for volume recombination in plane-parallel chambers in pulsed fields of high dose-per-pulse. Phys Med Biol. 2017;62(22):8634–54.

[89]   Bin JH, Ji Q, Seidl PA, Raftrey D, Steinke S, Persaud A, Nakamura K, Gonsalves A, Leemans WP, Schenkel T. Absolute calibration of GafChromic film for very high flux laser driven ion beams. Rev Sci Instrum. 2019;90:053301.

[90]   Richter C, Karsch L, Dammene Y, Kraft SD, Metzkes J, Schramm U, Schürer M, Sobiella M, Weber A, Zeil K, Pawelke J. A dosimetric system for quantitative cell irradiation experiments with laser-accelerated protons. Phys Med Biol. 2011;56(6):1529–43.

[91]   Zeil K, Baumann M, Beyreuther E, Burris-Mog T, Cowan TE, Enghardt W, Karsch L, Kraft SD, Laschinsky L, Metzkes J, Naumburger D, Oppelt M, Richter C, Sauerbrey R, Schürer M, Schramm U, Pawelke J. Dose-controlled irradiation of cancer cells with laser-accelerated proton pulses. Appl Phys B. 2013;110(4):437–44.

[92]   Esirkepov T, Borghesi M, Bulanov S V, Mourou G, Tajima T. Highly Efficient Relativistic-Ion Generation in the Laser-Piston Regime. Phys Rev Lett. 2004 Apr;92(17):175003.

[93]   Park J, Bulanov SS, Bin J, Ji Q, Steinke S, Vay JL, Geddes CGR, Schroeder CB, Leemans WP, Schenkel T, Esarey E. Ion acceleration in laser generated megatesla magnetic vortex. Phys Plasmas. 2019;26(10).

[94]   Fiuza F, Stockem A, Boella E, Fonseca RA, Silva LO, Haberberger D, Tochitsky S, Mori WB, Joshi C. Ion acceleration from laser-driven electrostatic shocks. Phys Plasmas. 2013;20(5):056304.

[95]   Leily Kiani, Tong Zhou, et al., "High average power ultrafast laser technologies for driving future advanced accelerators"; Whitepaper submission to Snowmass (AF6), 2022.

[96]   M. C. Vozenin, "Herman D. Suit Plenary Lecture - From irradiation at ultrahigh dose rate to FLASH radiotherapy: new radiobiology to support clinical translation," 67th Annual International Research Society, (Virtual), 2021.

[97]   S. Acharya, N. N. Bhat, P. Joseph, G. Sanjeev, B. Sreedevi and Y. Narayana, "Dose rate effect on micronuclei induction in human blood lymphocytes exposed to single

pulse and multiple pulses of electrons," Radiat Environ Biophys, vol. 50, p. 253–263, 2011.

[98]   K. Takayama and R. J. Briggs, Induction Accelerators, New York: Springer, 2011.

[99]   J. Barnard, R. Bangerter, A. Faltens, T. Fessenden, A. Friedman, E. Lee, B. Logan, S. Lund, W. Meier, W. Sharp and S. Yu,, "Induction accelerator architectures for heavy-ion fusion," Nucl. Instr. Meth. in Phys. Res. A, vol. 415, no. 1–2, pp. 218-228, 1998.

[100]   J. Smith, V. Bailey, H. Lackner and S. Putnam, "Performance of the spiral line induction accelerator," in Proceedings of the 1997 Particle Accelerator Conference, Vancouver, BC Canada, 1997.

[101]   S. E. Sampayan, K. C. Sampayan, G. J. Caporaso, Y.-J. Chen, S. Falabella, S. A. Hawkins, J. Hearn, J. A. Watson and J.-M. Zentler, "Megavolt bremsstrahlung measurements from linear induction accelerators demonstrate possible use as a FLASH radiotherapy source to reduce acute toxicity," Sci. Repts., vol. 11, p. 17104, 2021.

[102]   W. Panofsky and M. Bander, "Asymptotic theory of beam break-up in linear accelerators," Rev. Sci. Instr., vol. 39, no. 2, pp. 206-212, 1968.

[103]   S. Humphries, Charged Particle Beams, Hoboken, NJ: John Wiley and Sons, 1990.

[104]   I. Uetomi, M. Yamazaki, H. Kobayashi and I. Sato, "Extended Theory of Beam Loading in Electron Linac," Jpn. J. Appl. Phys., vol. 32, no. 6A, pp. 2858-2864, 1993.

[105]   L. G. Multhauf, N. L. Back, L. F. Simmons, J.-M. Zentler and R. D. Scarpetti, "Invited: The LLNL flash x-ray induction linear accelerator (FXR)," in Proc. SPIE 4948, 25th International Congress on High-Speed Photography and Photonics, Beaune, France, 2003.

[106]   W. E. Nexsen, D. P. Atkinson, D. M. Barrett, Y. J. Chen, J. C. Clark, L. V. Griffith, H. C. Kirbie, M. A. Newton, A. C. Paul, S. Sampayan, A. L. Throop and W. C. Turner, "The ETA-II induction LINAC as a high average power FEL driver," Nucl. Instrum. Meth. Phys. Res., vol. A296, pp. 54-61, 1990.

[107]   J. P. Negre and C. Rubbelynck, "Application of fast CVD diamond photoconductor detectors to MeV X-ray metrology for the AIRIX fash radiographic facility," Nucl. Instr. Meth. Phys. Res., vol. A 451, pp. 638-650, 2000.

[108]   M. Thumm, "State-of-the-Art of High-Power Gyro-Devices and Free Electron Masers," J. Infrared Milli Terahz Waves, vol. 41, p. 1–140, 2020.

[109]   C. D. Fryar, D. Kruszon-Moran, Q. Gu and C. L. Ogden, Mean body weight, height, waist circumference, and body mass index among adults: United States, 1999–2000 through 2015–2016, vol. 122, Washington, DC USA: United States Department of Health and Human Services, Centers for Disease Control and Prevention, 2018, pp. 1-15.

[110]   Durante M, Paganetti H. Nuclear physics in particle therapy: a review. Rep Prog
         Phys. 2016 Sep;79(9):096702. doi: 10.1088/0034-4885/79/9/096702. Epub 2016 Aug
         19. PMID: 27540827.

[111]   Svensson R, Brahme A. Effective source size, yield and beam profile from multi-
         layered bremsstrahlung targets. Phys Med Biol. 1996 Aug;41(8):1353-79. doi:
         10.1088/0031-9155/41/8/008. PMID: 8858725.

[112]   Wei S, Lin H, Choi JI, Simone CB 2nd, Kang M. A Novel Proton Pencil Beam
         Scanning FLASH RT Delivery Method Enables Optimal OAR Sparing and Ultra-
         High Dose Rate Delivery: A Comprehensive Dosimetry Study for Lung Tumors.
         Cancers (Basel). 2021 Nov 18;13(22):5790. doi: 10.3390/cancers13225790. PMID:
         34830946; PMCID: PMC8616118.

[113]   Kutsaev SV, Agustsson R, Arodzero A, Berry R, Bezhanov A, Boucher S,
         Chimalpopoca O, Diego A, Faillace L, Gavryushkin D, Harrison M, Hartzell JJ,
         McNevin J, Ruelas M, Yu Smirnov A, Verma A, Woods K. Compact X-Band
         Electron Linac for Radiotherapy and Security Applications. Radiat Phys Chem Oxf
         Engl 1993. 2021 Aug;185:109494. doi: 10.1016/j.radphyschem.2021.109494. Epub
         2021 Apr 11. PMID: 33935382; PMCID: PMC8081273.

[114]   Kutsaev, S. V. "Novel Technologies for Compact Electron Linear Accelerators
         (Review)." Instruments and experimental techniques (New York) 64.5 (2021): 641–
         656.

[115]   R. Agustsson, S. Boucher, and S. V. Kutsaev, "Linear accelerator for generating high
         x-ray doses," patent application WO2021113323A1, 2021.
         https://patentimages.storage.googleapis.com/e3/db/43/6f90567d69a1cc/WO20211133
         23A1.pdf

[116]   Lyu Q, Neph R, O'Connor D, Ruan D, Boucher S, Sheng K. ROAD: ROtational
         direct Aperture optimization with a Decoupled ring-collimator for FLASH
         radiotherapy. Phys Med Biol. 2021 Jan 29;66(3):035020. doi: 10.1088/1361-
         6560/abcbd0. PMID: 33207321; PMCID: PMC8683603.

[117]   Gao H, Lin B, Lin Y, Fu S, Langen K, Liu T, Bradley J. Simultaneous dose and dose
         rate optimization (SDDRO) for FLASH proton therapy. Med Phys. 2020
         Dec;47(12):6388-6395. doi: 10.1002/mp.14531. Epub 2020 Nov 8. PMID: 33068294.

[118]   Maxim PG, Tantawi SG, Loo BW Jr. PHASER: A platform for clinical translation of
         FLASH cancer radiotherapy. Radiother Oncol. 2019 Oct;139:28-33. doi:
         10.1016/j.radonc.2019.05.005. Epub 2019 Jun 6. PMID: 31178058.

[119]   Simmons DA, Lartey FM, Schüler E, Rafat M, King G, Kim A, Ko R, Semaan S,
         Gonzalez S, Jenkins M, Pradhan P, Shih Z, Wang J, von Eyben R, Graves EE, Maxim
         PG, Longo FM, Loo BW Jr. Reduced cognitive deficits after FLASH irradiation of
         whole mouse brain are associated with less hippocampal dendritic spine loss and
         neuroinflammation. Radiother Oncol. 2019 Oct;139:4-10. doi:
         10.1016/j.radonc.2019.06.006. Epub 2019 Jun 25. PMID: 31253467.

[120]   Schüler E, Trovati S, King G, Lartey F, Rafat M, Villegas M, Praxel AJ, Loo BW Jr, Maxim PG. Experimental Platform for Ultra-high Dose Rate FLASH Irradiation of Small Animals Using a Clinical Linear Accelerator. Int J Radiat Oncol Biol Phys. 2017 Jan 1;97(1):195-203. doi: 10.1016/j.ijrobp.2016.09.018. Epub 2016 Sep 20. PMID: 27816362.

[121]   Lagzda, A., Jones, R.M., Aitkenhead, A.H., Kirkby, K.J., MacKay, R.I., van Herk, M., Farabolini, W. and Corsini, R., 2018, June. Very-high energy electron (VHEE) studies at CERN'S CLEAR user facility. In Proc. 9th Int. Particle Accelerator Conf. doi:10.18429/JACoW-IPAC2018-MOPML023

[122]   Lempart M, Blad B, Adrian G, Bäck S, Knöös T, Ceberg C, Petersson K. Modifying a clinical linear accelerator for delivery of ultra-high dose rate irradiation. Radiother Oncol. 2019 Oct;139:40-45. doi: 10.1016/j.radonc.2019.01.031. Epub 2019 Feb 10. PMID: 30755324.

[123]   Rahman M, Ashraf MR, Zhang R, Bruza P, Dexter CA, Thompson L, Cao X, Williams BB, Hoopes PJ, Pogue BW, Gladstone DJ. Electron FLASH Delivery at Treatment Room Isocenter for Efficient Reversible Conversion of a Clinical LINAC. Int J Radiat Oncol Biol Phys. 2021 Jul 1;110(3):872-882. doi: 10.1016/j.ijrobp.2021.01.011. Epub 2021 Jan 11. PMID: 33444695.

[124]   Jaccard M, Durán MT, Petersson K, Germond JF, Liger P, Vozenin MC, Bourhis J, Bochud F, Bailat C. High dose-per-pulse electron beam dosimetry: Commissioning of the Oriatron eRT6 prototype linear accelerator for preclinical use. Med Phys. 2018 Feb;45(2):863-874. doi: 10.1002/mp.12713. Epub 2018 Jan 6. PMID: 29206287.

[125]   Lansonneur P, Favaudon V, Heinrich S, Fouillade C, Verrelle P, De Marzi L. Simulation and experimental validation of a prototype electron beam linear accelerator for preclinical studies. Phys Med. 2019 Apr;60:50-57. doi: 10.1016/j.ejmp.2019.03.016. Epub 2019 Mar 27. PMID: 31000086.

[126]   Felici, G., Barca, P., Barone, S., Bortoli, E., Borgheresi, R., De Stefano, S., Di Francesco, M., Grasso, L., Linsalata, S., Marfisi, D. and Pacitti, M., 2020. Transforming an IORT linac into a FLASH research machine: Procedure and dosimetric characterization. Frontiers in Physics, p.374. doi: 10.3389/fphy.2020.00374

[127]   Moeckli R, Gonçalves Jorge P, Grilj V, Oesterle R, Cherbuin N, Bourhis J, Vozenin MC, Germond JF, Bochud F, Bailat C. Commissioning of an ultra-high dose rate pulsed electron beam medical LINAC for FLASH RT preclinical animal experiments and future clinical human protocols. Med Phys. 2021 Jun;48(6):3134-3142. doi: 10.1002/mp.14885. Epub 2021 May 14. PMID: 33866565.

[128]   Di Martino, F., Barca, P., Barone, S., Bortoli, E., Borgheresi, R., De Stefano, S., Di Francesco, M., Faillace, L., Giuliano, L., Grasso, L. and Linsalata, S., 2020. FLASH radiotherapy with electrons: issues related to the production, monitoring, and

dosimetric characterization of the beam. Frontiers in Physics, p.481. doi: 10.3389/fphy.2020.570697

[129]   "PMB-Alcen Announces the Launch of FLASHKNiFE, the FLASH Radiotherapy System Dedicated to Clinical Trials," June 24, 2020. https://www.pmb-alcen.com/en/news/pmb-alcen-announces-launch-flashknife-flash-radiotherapy-system-dedicated-clinical-trials

[130]   "NOVAC 11: mobile IOeRT accelerator," 2020, S.I.T. Sordina IORT Technologies S.p.A. https://www.soiort.com/novac-11/

[131]   Papiez L, DesRosiers C, Moskvin V. Very high energy electrons (50-250 MeV) and radiation therapy. Technol Cancer Res Treat. 2002 Apr;1(2):105-10. doi: 10.1177/153303460200100202. PMID: 12622516.

[132]   Bazalova-Carter M, Qu B, Palma B, Hårdemark B, Hynning E, Jensen C, Maxim PG, Loo BW Jr. Treatment planning for radiotherapy with very high-energy electron beams and comparison of VHEE and VMAT plans. Med Phys. 2015 May;42(5):2615-25. doi: 10.1118/1.4918923. PMID: 25979053.

[133]   Wuensch, W., "The CHUV-CERN facility for FLASH treatment of large, deep-seated tumors: the DEFT (Deep Electron FLASH Therapy) facility," Nov. 30, 2021, Presentation at the FLASH Radiotherapy & Particle Therapy (FRPT) Conference 2021.

[134]   Han, Y., Golfe, A.F., Vallerand, C., Bai, B., Duchesne, P., Prezado, Y., Delorme, R., Poortmans, P., Favaudon, V., Fouillade, C. and Pouzoulet, F., 2019, November. Optics design and beam dynamics simulation for a Vhee radiobiology beam line at Prae accelerator. In Journal of Physics: Conference Series (Vol. 1350, No. 1, p. 012200). IOP Publishing. doi:10.1088/1742-6596/1350/1/012200

[135]   Tantawi, S., Nasr, M., Li, Z., Limborg, C. and Borchard, P., 2020. Design and demonstration of a distributed-coupling linear accelerator structure. Physical Review Accelerators and Beams, 23(9), p.092001.

[136]   Nasr, M., Nanni, E., Breidenbach, M., Weathersby, S., Oriunno, M. and Tantawi, S., 2021. Experimental demonstration of particle acceleration with normal conducting accelerating structure at cryogenic temperature. Physical Review Accelerators and Beams, 24(9), p.093201.

[137]   Z. D. Farkas, H. A. Hogg, G. A. Loew, and P. B. Wilson, SLED: A method of doubling SLAC's energy, in Proceedings of 9th International Conference on High Energy Accelerators (SLAC, 1974), p. 576.

[138]   P. B. Wilson, Z. D. Farkas, and R. D. Ruth, in Proceedings of the 22nd 1990 LINAC Conference, PAC-2007, Albuquerque, NM (IEEE, New York, 2007).

[139]   D. Farkas, Binary peak power multiplier and its application to linear accelerator design, IEEE Trans. Microwave Theory Tech. 34, 1036 (1986).

[140]   Wang, J.W., Tantawi, S.G., Xu, C., Franzi, M., Krejcik, P., Bowden, G., Condamoor, S., Ding, Y., Dolgashev, V., Eichner, J. and Haase, A., 2017. Development for a supercompact X-band pulse compression system and its application at SLAC. Physical Review Accelerators and Beams, 20(11), p.110401. DOI: 10.1103/PhysRevAccelBeams.20.110401

[141]   Franzi, M., Wang, J., Dolgashev, V. and Tantawi, S., 2016. Compact rf polarizer and its application to pulse compression systems. Physical Review Accelerators and Beams, 19(6), p.062002. DOI: 10.1103/PhysRevAccelBeams.19.062002

[142]   Bai, Mei, Tim Barklow, Rainer Bartoldus, Martin Breidenbach, Philippe Grenier, Zhirong Huang, Michael Kagan et al. "C $^ 3$: A" Cool" Route to the Higgs Boson and Beyond." arXiv preprint arXiv:2110.15800 (2021). https://arxiv.org/abs/2110.15800

[143]   Nanni, Emilio, Martin Breidenbach, Caterina Vernieeri et al. " C3 Demonstration Research and Development Plan." arXiv preprint arXiv: 2203.09076. https://arxiv.org/abs/2203.09076

[144]   Martínez-Rovira I, Fois G, Prezado Y. Dosimetric evaluation of new approaches in GRID therapy using nonconventional radiation sources. Med Phys. 2015 Feb;42(2):685-93. doi: 10.1118/1.4905042. PMID: 25652482.

[145]   Snively, E.C., Deering, K., & Nanni, E.A. (2021). mm-Wave Linac Design for Next Generation VHEE Cancer Therapy Systems. DOI:10.18429/JACOW-IPAC2021-THPAB171, https://accelconf.web.cern.ch/ipac2021/papers/thpab171.pdf

[146]   Nanni, E.A., Dolgashev, V.A., Haase, A., Neilson, J., Tantawi, S., Schaub, S.C., Temkin, R.J. and Spataro, B., 2017, July. Prototyping high-gradient mm-wave accelerating structures. In Journal of Physics: Conference Series (Vol. 874, No. 1, p. 012039). IOP Publishing. doi :10.1088/1742-6596/874/1/012039

[147]   Othman, M.A.K., Dolgashev, V.A., Haase, A.A., Jawla, S., Nanni, E.A., Neilson, J., Picard, J.F., Schaub, S.C., Spataro, B., Tantawi, S.G. and Temkin, R.J., 2019. Initial Results of High-Gradient Breakdown Tests for W-Band Accelerating Structures (No. thpgw080). SLAC National Accelerator Lab., Menlo Park, CA (United States). doi:10.18429/JACoW-IPAC2019-THPGW080, https://accelconf.web.cern.ch/ipac2019/papers/thpgw080.pdf

[148]   Snively, E., Othman, M. A. K., Deering, K., Kuppusamy, S., Wehner, G. T., and Nanni, E. A., "High Gradient mm-Wave Linac for VHEE Therapy," Dec. 3, 2021, Poster presentation at the FLASH Radiotherapy & Particle Therapy (FRPT) Conference 2021.

[149]   Kutsaev, S.V., Jacobson, B., Smirnov, A.Y., Campese, T., Dolgashev, V.A., Goncharik, V., Harrison, M., Murokh, A., Nanni, E., Picard, J. and Ruelas, M., 2019. Nanosecond rf-power switch for gyrotron-driven millimeter-wave accelerators. Physical Review Applied, 11(3), p.034052. https://doi.org/10.1103/PhysRevApplied.11.034052

[150]   Othman, M.A., Picard, J., Schaub, S., Dolgashev, V.A., Lewis, S.M., Neilson, J., Haase, A., Jawla, S., Spataro, B., Temkin, R.J. and Tantawi, S., 2020. Experimental demonstration of externally driven millimeter-wave particle accelerator structure. Applied Physics Letters, 117(7), p.073502. https://doi.org/10.1063/5.0011397

[151]   Lewis, S.M., Haase, A.A., Kim, D., Nanni, E.A., Othman, M.A.K., Simakov, E.I. and Sy, A.V., 2019. Design of a High Gradient THz-Driven Electron Gun (No. SAPAF04). SLAC National Accelerator Lab., Menlo Park, CA (United States). doi:10.18429/JACoW-IPAC2019-TUPTS077

[152]   Göbel, H. "Dose Delivery system of the Varian ProBeam System with Continuous Beam," Presentation at the EUCARD2 Workshop on Innovative Delivery Systems in Particle Therapy, Torino, Italy, Feb. 2017.

[153]   Lu, X., Li, Z., Dolgashev, V., Bowden, G., Sy, A., Tantawi, S. and Nanni, E.A., 2021. A proton beam energy modulator for rapid proton therapy. Review of Scientific Instruments, 92(2), p.024705. https://doi.org/10.1063/5.0035331

[154]   Pedroni E, Bacher R, Blattmann H, Böhringer T, Coray A, Lomax A, Lin S, Munkel G, Scheib S, Schneider U, et al. The 200-MeV proton therapy project at the Paul Scherrer Institute: conceptual design and practical realization. Med Phys. 1995 Jan;22(1):37-53. doi: 10.1118/1.597522. PMID: 7715569.

[155]   FlashForward Consortium. https://www.varian.com/about-varian/research/flashforward-consortium

[156]   Garcia, J.B., Calaga, R., De Maria, R., Giovannozzi, M., Grudiev, A. and Tomás, R., 2012. Study of Multipolar RF Kicks from the main deflecting mode in compact crab cavities for LHC. In 3rd International Particle Accelerator Conference. https://cds.cern.ch/record/1459579

[157]   Snively, E., Lu, X., Nanni, E., Li, Z., Dolgashev, V., Bowden, G., Sy, A. and Tantawi, S., 2020. Deflector Cavity Design for Rapid 2-D Proton Beam Scanning. Bulletin of the American Physical Society, 65.

[158]   Dasu, Sridhara, Emilio A. Nanni, Michael E. Peskin, Caterina Vernieri, Tim Barklow, Pushpalatha C. Bhat, Kevin Black et al. "Strategy for Understanding the Higgs Physics: The Cool Copper Collider." arXiv preprint arXiv:2203.07646 (2022).